

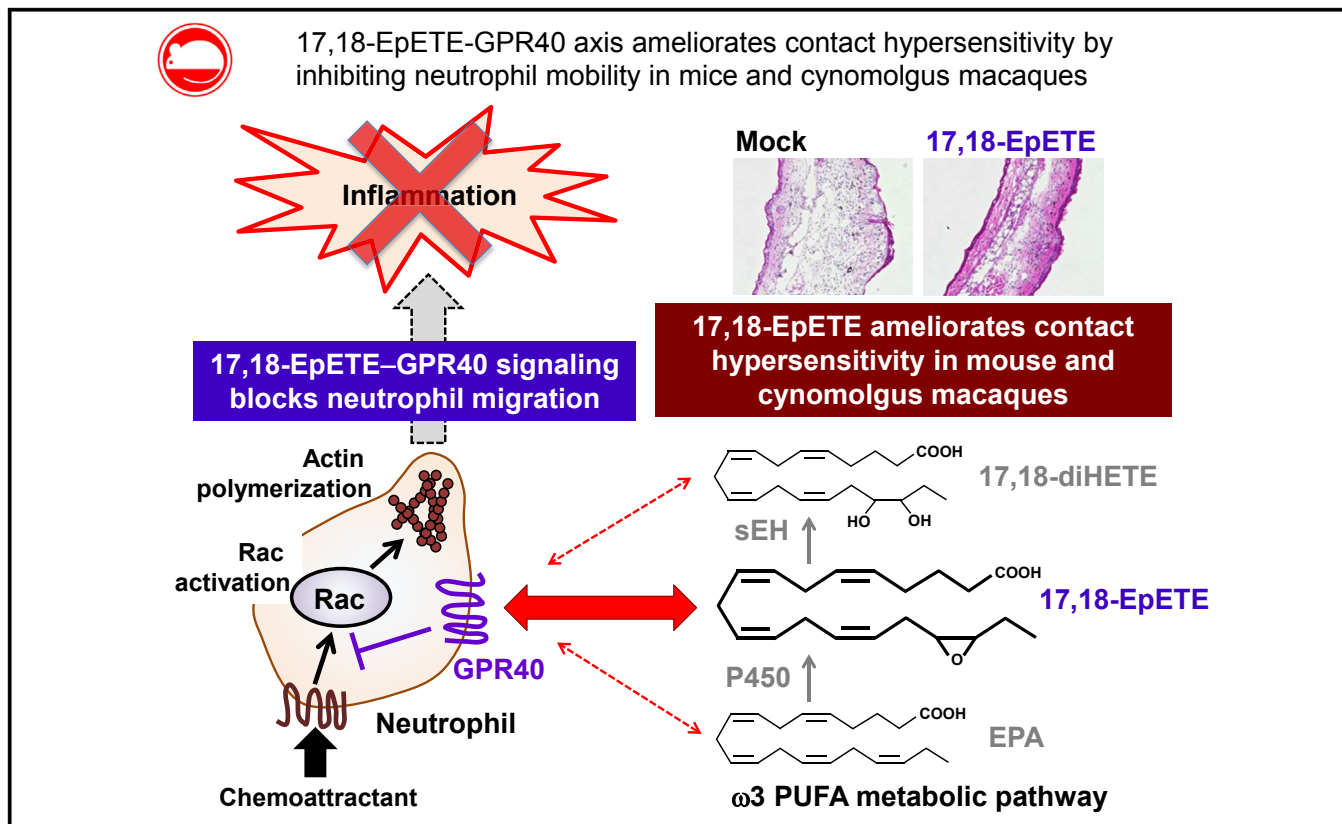
Title	The 17,18-epoxyeicosatetraenoic acid-G protein-coupled receptor 40 axis ameliorates contact hypersensitivity by inhibiting neutrophil mobility in mice and cynomolgus macaques
Author(s)	Nagatake, Takahiro; Shiogama, Yumiko; Inoue, Asuka; Kikuta, Junichi; Honda, Tetsuya; Tiwari, Prabha; Kishi, Takayuki; Yanagisawa, Atsushi; Isobe, Yosuke; Matsumoto, Naomi; Shimojou, Michiko; Morimoto, Sakiko; Suzuki, Hidehiko; Hirata, So-ichiro; Steneberg, Pär; Edlund, Helena; Aoki, Junken; Arita, Makoto; Kiyono, Hiroshi; Yasutomi, Yasuhiro; Ishii, Masaru; Kabashima, Kenji; Kunisawa, Jun
Citation	Journal of Allergy and Clinical Immunology (2018), 142(2): 470-484.e12
Issue Date	2018-08
URL	http://hdl.handle.net/2433/233926
Right	© 2017 The Authors. Published by Elsevier Inc. on behalf of the American Academy of Allergy, Asthma & Immunology. This is an open access article under the CC BY-NC-ND license (http://creativecommons.org/licenses/by-nc-nd/4.0/).
Type	Journal Article
Textversion	publisher

The 17,18-epoxyeicosatetraenoic acid–G protein–coupled receptor 40 axis ameliorates contact hypersensitivity by inhibiting neutrophil mobility in mice and cynomolgus macaques

Check for updates

Takahiro Nagatake, PhD,^a Yumiko Shiogama, DVM,^b Asuka Inoue, PhD,^c Junichi Kikuta, MD, PhD,^d Tetsuya Honda, MD, PhD,^e Prabha Tiwari, PhD,^a Takayuki Kishi, BSc,^c Atsushi Yanagisawa,^d Yosuke Isobe, PhD,^f Naomi Matsumoto, BSc,^a Michiko Shimojoui, MSc,^a Sakiko Morimoto, MSc,^a Hidehiko Suzuki, PhD,^a So-ichiro Hirata, MSc,^{a,g} Pär Steneberg, PhD,^h Helena Edlund, PhD,^h Junken Aoki, PhD,^c Makoto Arita, PhD,^{f,i,j} Hiroshi Kiyono, DDS, PhD,^{k,l} Yasuhiro Yasutomi, DVM, PhD,^{b,m} Masaru Ishii, MD, PhD,^d Kenji Kabashima, MD, PhD,^e and Jun Kunisawa, PhD^{a,g,k,n} Ibaraki, Tsukuba, Sendai, Suita, Kyoto, Kobe, Yokohama, Tokyo, Chiba, and Tsu, Japan, and Umea, Sweden

GRAPHICAL ABSTRACT



From ^athe Laboratory of Vaccine Materials, Center for Vaccine and Adjuvant Research, and Laboratory of Gut Environmental System, National Institutes of Biomedical Innovation, Health and Nutrition (NIBIOHN), Ibaraki; ^bthe Laboratory of Immunoregulation and Vaccine Research, Tsukuba Primate Research Center, NIBIOHN, Tsukuba; ^cthe Laboratory of Molecular and Cellular Biochemistry, Graduate School of Pharmaceutical Sciences, Tohoku University, Sendai; ^dthe Department of Immunology and Cell Biology, Graduate School of Medicine and Frontier Biosciences, and ^ethe Graduate School of Medicine, Graduate School of Pharmaceutical Sciences, Graduate School of Dentistry, Osaka University, Suita; ^fthe Department of Dermatology, Kyoto University Graduate School of Medicine, Kyoto; ^gthe Laboratory for Metabolomics, RIKEN Center for Integrative Medical Sciences, Yokohama; ^hthe Department of

Microbiology and Immunology, Kobe University Graduate School of Medicine, Kobe; ⁱUmea Center for Molecular Medicine, Umea University, Umea; ^jthe Graduate School of Medical Life Science, Yokohama City University, Tsurumi-ku, Yokohama; ^kthe Division of Physiological Chemistry and Metabolism, Graduate School of Pharmaceutical Sciences, Keio University, Minato-ku, Tokyo; ^lthe Division of Mucosal Immunology, Department of Microbiology and Immunology and International Research and Development Center for Mucosal Vaccines, Institute of Medical Science, University of Tokyo, Tokyo; ^mthe Department of Immunology, Graduate School of Medicine, Chiba University, Chiba; and ⁿthe Division of Immunoregulation, Department of Molecular and Experimental Medicine, Mie University Graduate School of Medicine, Tsu.

Background: Metabolites of eicosapentaenoic acid exert various physiologic actions. 17,18-Epoxyeicosatetraenoic acid (17,18-EpETE) is a recently identified new class of antiallergic and anti-inflammatory lipid metabolite of eicosapentaenoic acid, but its effects on skin inflammation and the underlying mechanisms remain to be investigated.

Objective: We evaluated the effectiveness of 17,18-EpETE for control of contact hypersensitivity in mice and cynomolgus macaques. We further sought to reveal underlying mechanisms by identifying the responsible receptor and cellular target of 17,18-EpETE.

Methods: Contact hypersensitivity was induced by topical application of 2,4-dinitrofluorobenzene. Skin inflammation and immune cell populations were analyzed by using flow cytometric, immunohistologic, and quantitative RT-PCR analyses. Neutrophil mobility was examined by means of imaging analysis *in vivo* and neutrophil culture *in vitro*. The receptor for 17,18-EpETE was identified by using the TGF- α shedding assay, and the receptor's involvement in the anti-inflammatory effects of 17,18-EpETE was examined by using KO mice and specific inhibitor treatment.

Results: We found that preventive or therapeutic treatment with 17,18-EpETE ameliorated contact hypersensitivity by inhibiting neutrophil mobility in mice and cynomolgus macaques. 17,18-EpETE was recognized by G protein-coupled receptor (GPR) 40 (also known as free fatty acid receptor 1) and inhibited

chemoattractant-induced Rac activation and pseudopod formation in neutrophils. Indeed, the antiallergic inflammatory effect of 17,18-EpETE was abolished in the absence or inhibition of GPR40. **Conclusion:** 17,18-EpETE inhibits neutrophil mobility through GPR40 activation, which is a potential therapeutic target to control allergic inflammatory diseases. (*J Allergy Clin Immunol* 2018;142:470-84.)

Key words: 17,18-Epoxyeicosatetraenoic acid, G protein-coupled receptor 40, ω 3 fatty acid, contact hypersensitivity, dermatitis, neutrophil

Omega-3 (ω 3) and ω 6 polyunsaturated fatty acids are essential fatty acids because they cannot be produced within the mammalian body and therefore must be ingested from the diet. The major ω 3 fatty acid in dietary oils is α -linolenic acid (ALA), which is particularly abundant in linseed and perilla oils.^{1,2} Fatty acid desaturase and elongase metabolize ALA into eicosapentaenoic acid (EPA) and docosahexaenoic acid (DHA), which are predominant in fish oils.^{1,2} Several lines of evidence have revealed that dietary intake of these oils shows antiallergic and/or anti-inflammatory properties.¹⁻⁵

Recent advances in lipidomics using liquid chromatography-tandem mass spectrometry have led to identification of a new class of lipid metabolites that play a pivotal role in the control of allergy and inflammation.⁶⁻⁸ These metabolites are derived from

Supported by grants from the Ministry of Education, Culture, Sports, Science, and Technology of Japan (MEXT) and the Japan Society for the Promotion of Science (JSPS; KAKENHI [JP15K19142 to T.N., JP17K08264 to A.I., JP15K09766 to T.H., JP17K08301 to H.S., JP15H05897 to J.A., JP15H04648 to M.A., JP15K15417 and JP15H02551 to K.K., JP15H05790 to K.K. and J.K., and JP26670241 and JP26293111 to J.K.]); the Japan Science and Technology Agency (JST), PRESTO (to A.I.; JPMJPR1331); the Japan Agency for Medical Research and Development (AMED; [JP17ek0410032h0002 to H.K., JP17gm5910013 to A.I., JP17gm0710001 to J.A. and JP17ek0410032s0102, JP17ek0210078h0002, JP17ak0101068h0001 and JP17gm1010006s0101 to J.K.]); the Ministry of Health and Welfare of Japan (to J.K.); the Science and Technology Research Promotion Program for Agriculture, Forestry, Fisheries, and Food Industry (to M.A. and J.K.); a grant-in-aid for Scientific Research on Innovative Areas from MEXT (JP15H05906 to T.H.; JP3701, JP15K21738, JP15H05898, and JP15H05897 to M.A.; JP15H01155 to K.K.; JP23116506 to H.K. and J.K.; and JP16H01373 and JP25116706 to J.K.); the Strategic Research Program in Diabetes at Umea University (to H.E. and P.S.); the Grant for Joint Research Project of the Institute of Medical Science, the University of Tokyo (to J.K.); the Astellas Foundation for Research on Metabolic Disorders (to J.K.); Terumo Foundation for Life Sciences and Arts (to J.K.); the Nipponham Foundation for the Future of Food; and the Suzuken Memorial Foundation (to J.K.); the Canon Foundation (to J.K.). Y.I. was supported by a RIKEN Special Postdoctoral Researcher Program. P.T. was supported by a fellowship from the Tokyo Biochemical Research Foundation and Takeda Science Foundation. T.K. was supported by a JSPS Research Fellowship.


Disclosure of potential conflict of interest: T. Nagatake, T. Kishi, and H. Suzuki have received grants from the Japan Society for the Promotion of Science. A. Inoue has received grants from the Japan Science and Technology Agency, the Japan Agency for Medical Research and Development, the Japan Society for the Promotion of Science, and Ono Medical Research Foundation and has a patent for a method for detecting signal transduction of G protein-coupled receptor (WO2015128894A1). T. Honda has received grants from the Ministry of Education, Culture, Sports, Science, and Technology of Japan; the Japan Society for the Promotion of Science; Mitsubishi Tanabe Pharma; Sanofi Japan Group; AbbVie GK; the Lydia O'Leary Memorial Dermatological Foundation; ROHTO Pharmaceutical; Shiseido; Novartis International AG; and Kao Co and has received payment for lectures from Novartis International AG, AbbVie GK, Sanofi Japan Group, Mitsubishi Tanabe Pharma, Janssen Pharma, Kyowa Hakkō Kirin, and Torii Pharmaceutical. P. Tiwari has received grants from the Tokyo Biochemical Research Foundation and Takeda Science Foundation. H. Edlund has a board membership with and receives stock/stock options from Betagenon AB. J. Aoki has received grants from the Japan Agency for Medical Research and Development; the Ministry of Education, Culture, Sports, Science, and

Technology of Japan; Ono Pharmaceutical; Kyorin Pharmaceutical; Astellas Pharma; the Japan Society for the Promotion of Science; and Tosoh and has a patent for a method for detecting signal transduction of G protein-coupled receptor (WO2015128894A1). M. Arita has received grants from the Ministry of Education, Culture, Sports, Science, and Technology of Japan; the Science and Technology Research Promotion Program for Agriculture, Forestry, Fisheries, and Food Industry; and the Japan Society for the Promotion of Science. H. Kiyono has received grants from the Ministry of Education, Culture, Sports, Science, and Technology of Japan and the Japan Agency for Medical Research and Development and is employed by the University of Tokyo, Chiba University, and the Japan Society for the Promotion of Science. K. Kabashima has received grants from the Japan Society for the Promotion of Science, Sanofi Japan Group, Mitsubishi Tanabe Pharma, Chugai Pharmaceutical, Pola Pharma, Maruho, and the Ministry of Education, Culture, Sports, Science, and Technology of Japan; has received payment for lectures from Pola Pharma, Kyowa Hakkō Kirin, Maruho, and Leo Pharma; and has received payment for writing the manuscript from Sanofi Japan Group. J. Kunisawa has received grants from the Ministry of Education, Culture, Sports, Science, and Technology of Japan; the Japan Agency for Medical Research and Development; the Ministry of Health and Welfare of Japan; the Science and Technology Research Promotion Program for Agriculture, Forestry, Fisheries, and Food Industry; the Japan Society for the Promotion of Science; the Astellas Foundation for Research on Metabolic Disorders; the Terumo Foundation for Life Sciences and Arts; the Nipponham Foundation for the Future of Food; Suzuken Memorial Foundation; Ono Pharmaceutical; MGP; Nitto Pharma; Morinaga Milk; and Nippon Flour Mills; has consultant arrangements with EA Pharma, Suntory Holdings, and Ono Pharmaceutical. The rest of the authors declare that they have no relevant conflicts of interest.

Received for publication February 10, 2017; revised August 2, 2017; accepted for publication September 14, 2017.

Available online December 27, 2017.

Corresponding author: Jun Kunisawa, PhD, Laboratory of Vaccine Materials, Center for Vaccine and Adjuvant Research and Laboratory of Gut Environmental System, NIBIOHN, 7-6-8 Asagi Saito, Ibaraki, Osaka 567-0085, Japan. E-mail: kunisawa@nibiohn.go.jp.

 The CrossMark symbol notifies online readers when updates have been made to the article such as errata or minor corrections
0091-6749

© 2017 The Authors. Published by Elsevier Inc. on behalf of the American Academy of Allergy, Asthma & Immunology. This is an open access article under the CC BY-NC-ND license (<http://creativecommons.org/licenses/by-nc-nd/4.0/>).

<https://doi.org/10.1016/j.jaci.2017.09.053>

Abbreviations used

ALA:	α -Linolenic acid
APC:	Allophycocyanin
Chi3l3:	Chitinase 3-like 3
CYP:	Cytochrome P450
DAPI:	4'-6-Diamidino-2-phenylindole dihydrochloride
DC:	Dendritic cell
DNFB:	2,4-Dinitrofluorobenzene
DHA:	Docosahexaenoic acid
17,18-diHETE:	17,18-Dihydroxy-eicosa-5,8,11,14-tetraenoic acid
EPA:	Eicosapentaenoic acid
17,18-EpETE:	17,18-Epoxyeicosatetraenoic acid
FasL:	Fas ligand
FITC:	Fluorescein isothiocyanate
fMLP:	N-formyl-methionyl-phenylalanine
GPR:	G protein-coupled receptor
G-CSF:	Granulocyte colony-stimulating factor
HEK293:	Human embryonic kidney 293
ICAM:	Intercellular adhesion molecule
iSALT:	Inducible skin-associated lymphoid tissue
NIBIOHN:	National Institutes of Biomedical Innovation, Health and Nutrition
PE:	Phycoerythrin
PPAR:	Peroxisome proliferator-activated receptor

EPA (eg, E-series resolvins) and DHA (D-series resolvins, maresins, and protectins) and are generated through the combined activity of COX-2, lipoxygenase, and cytochrome P450 (CYP), which are central to various diseases, including intestinal inflammation, rheumatoid arthritis, asthma, diabetes, and atherosclerosis.⁶⁻⁸

Recently, we showed that feeding mice a diet containing linseed oil (also known as flaxseed oil), a dietary oil enriched in ALA, ameliorated ovalbumin-induced allergic diarrhea.⁹ Lipidomics analysis revealed that concentrations of 17,18-epoxyeicosatetraenoic acid (17,18-EpETE) were increased significantly in the intestines of mice maintained on the linseed oil diet. Furthermore, intraperitoneal administration of synthetic 17,18-EpETE inhibited the development of food allergy in mice.⁹ Separate studies demonstrated that 17,18-EpETE and its hydroxyl derivative, 12-OH-17,18-EpETE, were also effective for the control of other allergic and inflammatory diseases, such as asthma,¹⁰ choroidal neovascularization,¹¹ and peritonitis.¹²

These findings suggest collectively that 17,18-EpETE is a new EPA metabolite that can be used to control allergic and inflammatory diseases; however, its effects on skin inflammation and the molecular and cellular mechanisms underlying the anti-allergic and anti-inflammatory properties of 17,18-EpETE remain to be investigated. The anti-inflammatory effects of 17,18-EpETE are mediated by nuclear receptor of peroxisome proliferator-activated receptor (PPAR) γ .¹⁰ In addition to nuclear receptors, G protein-coupled receptors (GPRs) act as cell-surface receptors for several types of free fatty acids. For example, GPR41 and GPR43 are activated by short-chain fatty acids, such as acetate, propionate, and butyrate.¹³ GPR84 acts as a receptor for medium-chain fatty acids, such as capric acid and lauric acid.¹⁴ GPR40 and GPR120 respond to long-chain fatty acids, including palmitic acid, EPA, and DHA.^{15,16} However, it remains unclear which receptors are activated by 17,18-EpETE.

The incidence of allergic and inflammatory skin diseases is increasing worldwide.^{17,18} Contact dermatitis is a major allergic

skin disease that affects 15% to 20% of the world's population.¹⁸ Murine models of contact dermatitis are well established as contact hypersensitivity and have revealed the molecular and cellular immunopathologic pathways in the sensitization and elicitation phases of the disease.¹⁹ In the sensitization phase of contact hypersensitivity, keratinocytes are activated in response to exposure to an allergen or hapten and consequently produce inflammatory mediators, such as prostaglandin E₂, TNF- α , and IL-1 β . These mediators induce the maturation of skin dendritic cells (DCs) and their migration to draining lymph nodes, where DCs activate naive T cells for the generation of allergen-specific effector or pathologic T cells.¹⁹ In the elicitation phase of contact hypersensitivity, neutrophils and memory T cells expressing CXCR2 and CXCR3, respectively, infiltrate into the skin in response to chemokines and adhesion molecules, including the neutrophil attractants CXCL1 and CXCL2 and the T-cell attractants CXCL9, CXCL10, and intercellular adhesion molecule (ICAM) 1 in the context of increased vascular permeability.¹⁹ Granulocyte colony-stimulating factor (G-CSF) contributes to neutrophil infiltration also.²⁰ In addition, B cells play a role in the recruitment of T cells by producing IgM antibody, which induces complement activation and mast cell degranulation.²¹ On infiltration into the skin, T cells are further activated by cutaneous antigen-presenting cells and produce inflammatory cytokines (eg, IFN- γ and IL-17A). Indeed, the depletion of neutrophils by using cell-specific antibody^{20,22,23} or, alternatively, gene deletion of IFN- γ ²⁴ or IL-17A²⁵ impairs the development of contact hypersensitivity. A recent study has shown that formation of clusters of DCs in the skin, known as inducible skin-associated lymphoid tissue (iSALT), is induced by macrophages and plays an important role in the activation and proliferation of memory T cells during the elicitation phase.²⁶

Despite the numerous detailed studies on allergic skin inflammation, currently approved medicines against skin inflammation include only steroids and immunosuppressants (eg, calcineurin inhibitors).¹⁷ Because side effects of these drugs include skin thinning and infectious diseases, new types of immunotherapy and medicines with high safety and efficacy are needed. In this context several recent studies have indicated the possible application of lipid mediators for the control of skin inflammation. For example, treatment of mice with resolvin E1, an EPA-derived metabolite, attenuated skin inflammation.^{27,28} Therefore lipid mediators appear to be promising targets for the treatment of allergic skin inflammation, including contact dermatitis. In the current study we evaluated the effects of 17,18-EpETE on the treatment of contact hypersensitivity in mice and cynomolgus macaques and investigated the molecular and cellular mechanisms underlying its anti-allergic and anti-inflammatory properties.

METHODS**Animals**

Female wild-type C57BL/6 mice (age 6-8 weeks) were purchased from Japan SLC (Hamamatsu, Japan) or CLEA Japan (Tokyo, Japan) and kept for at least 1 week before experiments in the specific pathogen-free animal facility at the National Institutes of Biomedical Innovation, Health and Nutrition (NIBIOHN; Osaka, Japan). *Ffar1*^{-/-} mice were generated previously¹⁶ and bred and maintained in the animal facility at NIBIOHN. Mice were killed by means of cervical dislocation after achievement of anesthesia with isoflurane (Foranel AbbVie, North Chicago, Ill). For the pharmacokinetic analysis, 6-week-old male Crl:CD (SD) rats received 17,18-EpETE (2 mg/kg administered orally). Plasma samples were collected at 0.25, 0.5, 1, 2, 4, 8, and 24 hours after administration, and the amount of 17,18-EpETE was measured by using

liquid chromatography–tandem mass spectrometry.⁹ Female cynomolgus macaques (*Macaca fascicularis*; age, 14–22 years; weight, 2–3 kg) were maintained at the Tsukuba Primate Research Center, NIBIOHN, according to the “Rules for animal care and management of Tsukuba Primate Center”²⁹ and the “Guiding principles for animal experiments using nonhuman primates” formulated by the Primate Society of Japan. All experiments were conducted in accordance with the guidelines of the Animal Care and Use Committee of NIBIOHN and Osaka University and the Committee on the Ethics of Animal Experiments of NIBIOHN and Osaka University (DS25-2, DS25-3, and DS26-41).

Bone marrow transplantation

Bone marrow cells were prepared from the femurs and tibiae of 8-week-old donor mice. Recipient mice (age, 6 weeks) were X-irradiated (dose, 8 Gy; MBR-1520R-3; Hitachi, Tokyo, Japan) 6 hours before injection of bone marrow cells (1×10^7 cells per recipient) into the tail vein. Transplanted recipient mice were allowed to recover for at least 8 weeks before their use in experiments.

Induction of contact hypersensitivity in mice

Contact hypersensitivity was induced, as described previously with modifications.²⁶ Briefly, the abdominal skin of each mouse was shaved and then treated with 25 μ L of 0.5% (vol/vol) 2,4-dinitrofluorobenzene (DNFB; Nacalai Tesque [Kyoto, Japan] or Sigma [St Louis, Mo]) dissolved in a mixture of acetone (Nacalai Tesque or Wako [Tokyo, Japan]) and olive oil (Nacalai Tesque or Wako; acetone/olive oil, 4:1). After 5 days, the fronts and backs of both ears were challenged with 0.2% (vol/vol) DNFB (10 μ L per site). At 48 hours after DNFB treatment, ear thickness was measured with a micrometer (model MDC-25MJ 293-230; Mitsutoyo, Kawasaki, Japan). Mice received 17,18-EpETE (dose: 100 ng administered intraperitoneally or 1 μ g administered orally or topically; Cayman Chemical, Ann Arbor, Mich), 17,18-dihydroxy-eicosa-5,8,11,14-tetraenoic acid (17,18-diHETE; dose: 100 ng administered intraperitoneally; Cayman Chemical), TAK-875 (dose: 60 μ g administered intraperitoneally; ChemScene, Monmouth Junction, NJ), resolvin E1 (dose: 200 ng administered intraperitoneally; Cayman Chemical), or 0.5% (vol/vol) ethanol dissolved in PBS as a vehicle control 30 minutes before DNFB stimulation. In some experiments mice received GW1100 (1 mg/kg administered intraperitoneally; Focus Biomolecules, Plymouth Meeting, Pa) 30 minutes before 17,18-EpETE treatment. In some experiments mice were topically treated with dexamethasone (Tokyo Chemical Industry, Tokyo, Japan), as described previously with modifications.³⁰ In brief, abdominal skin (25 μ L) and ears (10 μ L per site) were topically treated with 0.12% (vol/vol) dexamethasone at days 0 and 5, respectively, 30 minutes before stimulation with DNFB.

Induction of contact hypersensitivity in cynomolgus macaques

The abdominal skin of cynomolgus macaques was clipped free of hair and then sensitized with 2.5 mL of 0.5% (vol/vol) DNFB dissolved in a mixture of acetone and olive oil (ratio, 4:1). After 5 days, the dorsal skin was shaved and challenged with 700 μ L of 0.2% (vol/vol) DNFB; 48 hours later, each animal was treated with 17,18-EpETE (150 μ g administered topically) or vehicle. Skin samples were obtained by means of biopsy 72 hours after 17,18-EpETE application.

Cell isolation and flow cytometric analysis

Cell isolation and flow cytometry were performed, as described previously with modification.²⁸ The ears were split into dorsal and ventral skin, and the cartilage was removed by scratching with tweezers. Skin was cut into small pieces by using scissors and incubated in 2 mg/mL collagenase (Wako) in RPMI 1640 medium (Sigma-Aldrich) containing 2% (vol/vol) newborn calf serum (Equitech-Bio, Kerrville, Tex) for 60 to 90 minutes at 37°C with stirring. Cell suspensions were filtered through cell strainers (pore size, 70 μ m; BD Biosciences, Franklin Lakes, NJ) and stained with an anti-CD16/32

mAb (TruStain fcX; BioLegend, San Diego, Calif; 101320; 1:100) to avoid nonspecific staining. Cells were further stained with the following fluorescently labeled mAbs: fluorescein isothiocyanate (FITC)–anti-Ly6G (BioLegend; 127606; 1:100), FITC–anti-Gr1 (BioLegend; 108406, 1:100), allophycocyanin (APC)–Cy7–anti-CD11b (BioLegend; 101226; 1:100), phycoerythrin (PE)–Cy7–anti-CD11c (BioLegend; 117318; 1:100), PE–Cy7–anti-F4/80 (BioLegend; 123114; 1:100), PE–anti-F4/80 (BioLegend; 123110; 1:100), PE–anti-Langerin (Thermo Fisher Scientific, Waltham, Mass; 12-2075-82, 1:100), Alexa Fluor 647–anti-I-A^b (BioLegend; 116412; 1:100), Alexa Fluor 647–anti-Siglec-F (BD Biosciences; 562680, 1:100), PE–anti-c-Kit (BD Biosciences; 553355, 1:100), APC–anti-Fc ϵ RI (Thermo Fisher Scientific; 17-5898-82, 1:100), PE–anti-CD19 (BD Biosciences; 557399, 1:100), PE–Cy7–anti-B220 (BD Biosciences; 552772, 1:100), PE–anti-CD18 (BD Biosciences; 553293; 1:100), PE–rat IgG_{2a} isotype control (BD Biosciences; 553930, 1:100), PE–anti-CXCR2 (R&D Systems, Minneapolis, Minn; FAB2164P; 1:10), BV421–anti-CD3 ϵ (BioLegend; 100336, 1:100), BV421–anti-CD45 (BioLegend; 103133, 1:100), BV421–anti-CD11c (BioLegend; 117330, 1:25), BV421–anti-F4/80 (BioLegend; 123124, 1:100), APC–Annexin V (BioLegend; 640919; 1:20), PE–anti-Ki67 (BioLegend; 652404; 1:100), PE–anti-Fas ligand (FasL; BD Biosciences; 555293, 1:100), PE–hamster IgG₁ isotype control (BD Biosciences; 553972, 1:100), APC–anti-perforin (Thermo Fisher Scientific; 17-9392, 1:40), APC–rat IgG_{2a} isotype control (BioLegend; 400512, 1:40), FITC–anti-CD45 (BD Biosciences; 553079; 1:100), peridinin-chlorophyll-protein complex–anti-CD4 (BioLegend; 100432; 1:100), PE–anti-IFN- γ (BioLegend; 505808; 1:100), PE–rat IgG₁ isotype control (BioLegend; 401906, 1:100), BV421–anti-T-cell receptor β (BioLegend; 109230; 1:100), and Alexa Fluor 647–anti-IL-17A (BD Biosciences; 560184; 1:100).

Cells were treated for 60 minutes with brefeldin A (BioLegend) during collagenase treatment to stain intracellular cytokines. After viability and cell-surface markers were stained, cells were fixed and permeabilized (Cytofix/Cytoperm Fixation/Permeabilization Kit; BD Biosciences), according to the manufacturer’s protocol. Dead cells were detected by using Via-Probe (BD Biosciences; 555816), 7-aminoactinomycin D (BioLegend; 420404; 1:100), or Zombie-NIR Fixable Viability Kit; 423106; 1:100) and excluded from analysis. Samples were analyzed (MACSQuant [Miltenyi Biotec, Bergish Gladbach, Germany] or FACSARIA [BD Biosciences]), and cells were isolated (FACSARIA) by using flow cytometry. Data were analyzed with FlowJo 9.9 software (TreeStar, Ashland, Ore).

Reverse transcription and quantitative PCR analysis

Total RNA was isolated from purified cells by using Sepazol (Nacalai Tesque) and chloroform (Nacalai Tesque), precipitated with 2-propanol (Nacalai Tesque), and washed with 75% (vol/vol) ethanol (Nacalai Tesque). RNA samples were incubated with DNase I (Invitrogen, Carlsbad, Calif) to remove contaminating genomic DNA and then reverse transcribed into cDNA (Superscript III reverse transcriptase, VIRO cDNA Synthesis Kit; Invitrogen).

Ears were placed in XXTuff microvials (BioSpec Products, Bartlesville, Okla) containing 800 μ L of PBS and crushed by using stainless-steel beads (4.8 ϕ and 3.2 ϕ , TOMY) for 5 pulses (4800 rpm, 10 seconds each; Minibead-beater, BioSpec Products) to isolate RNA from ear tissues; samples were put on ice for 10 seconds between pulses. Samples were centrifuged (9100g for 20 minutes at 4°C), and the supernatant was processed to obtain total RNA (Relia Prep RNA Tissue Miniprep System; Promega, Tokyo, Japan), which was reverse transcribed, as described for purified cells.

Quantitative PCR analysis was performed with LightCycler 480 II (Roche, Basel, Switzerland) with FastStart Essential DNA Probes Master (Roche) or SYBR Green I Master reagents (Roche). Primer sequences were as follows: cathelicidin sense, 5'-gacaccaatctctacgctcc-3'; cathelicidin antisense, 5'-cacagactgggagatctgga-3'; β -defensin 1 sense, 5'-ggctgccaccactatgaaa-3'; β -defensin 1 antisense, 5'-tgtgagaatgccacacctg-3'; β -defensin 2 sense, 5'-tgctgctctcttctcatatac-3'; β -defensin 2 antisense, 5'-tcaagtctgctctgatatcca-3'; *Tnfa* sense, 5'-ctgtagccaccagctgtagc-3'; *Tnfa* antisense, 5'-ttgagatccatgccgttg-3'; chitinase 3–like 3 (*Chi3l3*) sense, 5'-aagaacactgagctaaaactctct-3'; *Chi3l3* antisense, 5'-gagaccatggcactgaagc-3'; *Cxcl1* sense, 5'-gactccagccactccaac-3'; *Cxcl1* antisense, 5'-tgacagcgcagctcattg-3';

Cxcl2 sense, 5'-aaaatcatccaaaagatactgaacaa-3'; *Cxcl2* antisense, 5'-ctttggttcctccgttgagg-3'; *G-CSF* sense, 5'-cctggagcaagtgaggaaga-3'; *G-CSF* antisense, 5'-gggtgtcacacagcttgtagg-3'; *Ffar1* sense, 5'-taggactggctctgtgct-3'; *Ffar1* antisense, 5'-ctgcagagaaaagaatgcacaa-3'; *Il10* sense, 5'-cagagccacagtctcctaga-3'; *Il10* antisense, 5'-tgtccagctggtctctgtt-3'; *Actb* sense, 5'-aaggccaacctgaaaagat-3'; and *Actb* antisense, 5'-gtgtgacagcaggagcaca-3'.

Histologic analysis

Frozen tissue was analyzed histologically, as described previously with some modification.³¹ Ear samples were washed with PBS (Nacalai Tesque) on ice and frozen in Tissue-Tek OCT compound (Sakura Finetek, Tokyo, Japan) in liquid nitrogen. Frozen tissue sections (6 μ m) were prepared by using a cryostat (model CM3050 S) and fixed for 30 minutes at 4°C in prechilled 95% ethanol (Nacalai Tesque), followed by 1 minute at room temperature in prechilled 100% acetone (Nacalai Tesque).

For staining with hematoxylin and eosin, tissue sections were washed with running water for 10 minutes, stained with Mayer hematoxylin solution (Wako) for 10 minutes, and washed with running water for 30 minutes. Tissue sections were then stained with 1% eosin Y solution (Wako) for 1 minute, washed with running water for 10 seconds, and dehydrated through increasing concentrations of ethanol (1 minute at each concentration, 70% to 100%; Nacalai Tesque). Tissue sections underwent final dehydration in xylene (Nacalai Tesque) for 3 minutes and were mounted in Permount (Falma, Tokyo, Japan).

For immunohistologic analysis, tissue sections were washed with PBS for 10 minutes and then blocked in 2% (vol/vol) newborn calf serum in PBS for 30 minutes at room temperature in an incubation chamber (Cosmo Bio, Tokyo, Japan). Tissue sections were incubated with primary antibodies in 2% (vol/vol) newborn calf serum in PBS for 16 hours at 4°C in the incubation chamber, washed once for 5 minutes each in 0.1% (vol/vol) Tween-20 (Nacalai Tesque) in PBS and PBS only, and then stained with secondary antibodies in 2% (vol/vol) newborn calf serum in PBS for 30 minutes at room temperature in the incubation chamber. To visualize nuclei, tissue sections then were washed twice (5 minutes each) with PBS and stained with 4'-6-diamidino-2-phenylindole dihydrochloride (DAPI; 1 μ mol/L; AAT Bioquest, Sunnyvale, Calif) for 10 minutes at room temperature in the incubation chamber. Finally, tissue sections were washed twice with PBS, mounted in Fluoromount (Diagnostic BioSystems, Pleasanton, Calif), and examined under a fluorescence microscope (model BZ-9000; Keyence, Osaka, Japan).

Paraffinated sections were trimmed to a thickness of 5 μ m by using a sliding microtome (model SM2010R; Leica Biosystems, Wetzlar, Germany) and subsequently deparaffinized by incubating in xylene (Nacalai Tesque) for 5 minutes, followed by rehydration through decreasing concentrations of ethanol (Nacalai Tesque) from 100% to 70% (1 minute at each concentration) at room temperature. Deparaffinized sections were stained with hematoxylin and eosin, as described above. For staining with an anti-CD66abce antibody, antigen retrieval was conducted by heating sections in 10 mmol/L sodium citrate (pH 6.0) for 10 minutes in a microwave oven before deparaffinization.

For histologic analysis, the following antibodies and reagents were used: purified anti-CD11c mAb (BioLegend; 117302; 1:50); purified anti-CD45 mAb (BioLegend; 103102; 1:100); purified anti-CD3e mAb (BioLegend; 100302; 1:100); Cy3-anti-Armenian hamster IgG (Jackson ImmunoResearch Laboratories, West Grove, Pa; 127-165-160; 1:200), Alexa Fluor 488-anti-rat IgG (Thermo Fisher Scientific; A-11006; 1:200), FITC-anti-Ly6G mAb (BioLegend; 127606; 1:100), biotin-anti-human CD66abce (Miltenyi Biotec; 130093156; 1:10), and FITC-streptavidin (BD Biosciences; 554060; 1:100). Cell nuclei were visualized by staining with DAPI (1 μ mol/L; AAT Bioquest), as described above.

In vivo labeling of neutrophils

Intravascular labeling of neutrophils was performed, as described previously with modification.^{32,33} In the DNFB-induced contact hypersensitivity model on day 7, mice were injected intravenously with 1 μ g of FITC-anti-Ly6G mAb in PBS containing 1 mmol/L CaCl₂ (Nacalai Tesque); 30 minutes after injection, cells were isolated from ears and examined by using flow cytometry.

In vitro neutrophil assay

The Rac activation assay was performed as previously described with modification.³⁴ Briefly, bone marrow-derived neutrophils were harvested by using 70% Percoll and cultured in RPMI1640 medium containing 50 μ mol/L 2-mercaptoethanol (Life Technologies, Carlsbad, Calif), 10 mmol/L HEPES (Nacalai Tesque), 0.5% BSA (Nacalai Tesque), and 100 μ g/mL penicillin-streptomycin (Nacalai Tesque). Cultured neutrophils were treated with either 17,18-EpETE (100 nmol/L) or ethanol (vehicle) for 15 minutes, followed by stimulation with 1 μ mol/L N-formyl-methionyl-phenylalanine (fMLP; Sigma-Aldrich) for 1 minute at 37°C. After stimulation, neutrophils were collected and lysed in 500 μ L of lysis buffer (20 mmol/L HEPES [pH 7.4], 150 mmol/L NaCl, 1% Triton X-100, 4 mmol/L EDTA, and 4 mmol/L EGTA) containing a protease-inhibitor cocktail (Sigma-Aldrich). The amount of protein in each sample was quantified by using the BCA Protein Assay Kit (Thermo Fisher Scientific). The volume of lysate containing 40 μ g of protein was incubated with 5 μ g of PAK1 PBD beads (Cell Biolabs, San Diego, Calif) for 30 minutes at 4°C with rotation. The beads were then washed 3 times with lysis buffer and resuspended in Nu-PAGE sample buffer (Invitrogen) containing a reducing agent (Invitrogen). The resulting bead-purified samples and whole-cell lysates were analyzed by means of Western blotting with Nu-PAGE 4%-12% gels (Invitrogen), anti-Rac 1/2/3 polyclonal antibody (Cell Signaling, Tokyo, Japan; 2465; 1:2500), anti-mouse β -actin (BioLegend; 643802; 1:1000), horseradish peroxidase-conjugated donkey anti-rabbit IgG (BioLegend; 406401; 1:2500), and goat anti-mouse IgG (SouthernBiotech, Birmingham, Ala; 1030-05; 1:8000). Western blot signals were detected by using an image analyzer (model LAS-4000, ImageQuant; GE Healthcare, Little Chalfont, United Kingdom).

For the F-actin polymerization assay, purified neutrophils (4×10^5 cells) were suspended in HBSS containing 0.2% BSA and allowed to adhere to fibronectin-coated coverslips (neuVibro, Vancouver, Wash) for 15 minutes in 5% CO₂ incubation. Neutrophils were treated with either 17,18-EpETE (20 nmol/L) or ethanol (vehicle) for 15 minutes and then stimulated with 1 μ mol/L fMLP for 2 minutes in 5% CO₂ incubation. Neutrophils were fixed with 4% paraformaldehyde (Nacalai Tesque), permeabilized with 0.5% Triton X-100 (Nacalai Tesque) in PBS, and stained in 100 nmol/L Acti-stain 488 phalloidin (Cytoskeleton, Denver, Colo) for 30 minutes at room temperature. Finally, cell nuclei were stained by incubating neutrophils in DAPI for 30 seconds at room temperature, and images were recorded (model TCS SP8; Leica Microsystems, Wetzlar, Germany).

ELISA for G-CSF

The amount of G-CSF protein in the serum was analyzed by using a Mouse G-CSF ELISA Kit (R&D Systems). Absorbance at OD₄₅₀ and OD₅₇₀ was measured by with the iMark microplate reader (Bio-Rad Laboratories, Hercules, Calif).

ELISA for IgM antibody

The amount of serum IgM antibody was analyzed by using ELISA, as described previously with modification.³⁵ In brief, serum was prepared from blood by means of centrifugation (5800g for 10 minutes). Supernatant was used for ELISA as a serum sample. Nunc MaxiSorp flat-bottom 96-well plates (Thermo Fisher Scientific) were coated with goat anti-mouse immunoglobulin (H+L; Southern Biotech; 1010-01, 1:1000). Serum samples diluted serially with PBS containing 1% (wt/vol) BSA were applied to the plates. IgM antibody was detected by using anti-mouse IgM-horseradish peroxidase (Southern Biotech; 1020-05, 1:4000) and visualized by adding TMB microwell peroxidase substrate (SeraCare Life Sciences, Milford, Mass). Thirty minutes after incubation, 0.5 mol/L HCl (Nacalai Tesque) was added, and absorbance at OD₄₅₀ was measured with the iMark microplate reader (Bio-Rad Laboratories).

TGF- α shedding assay

The TGF- α shedding assay was performed, as described previously.³⁶ In principle, activation of GPR was measured as ectodomain shedding of a membrane-bound proform of alkaline-phosphatase-tagged TGF- α and its

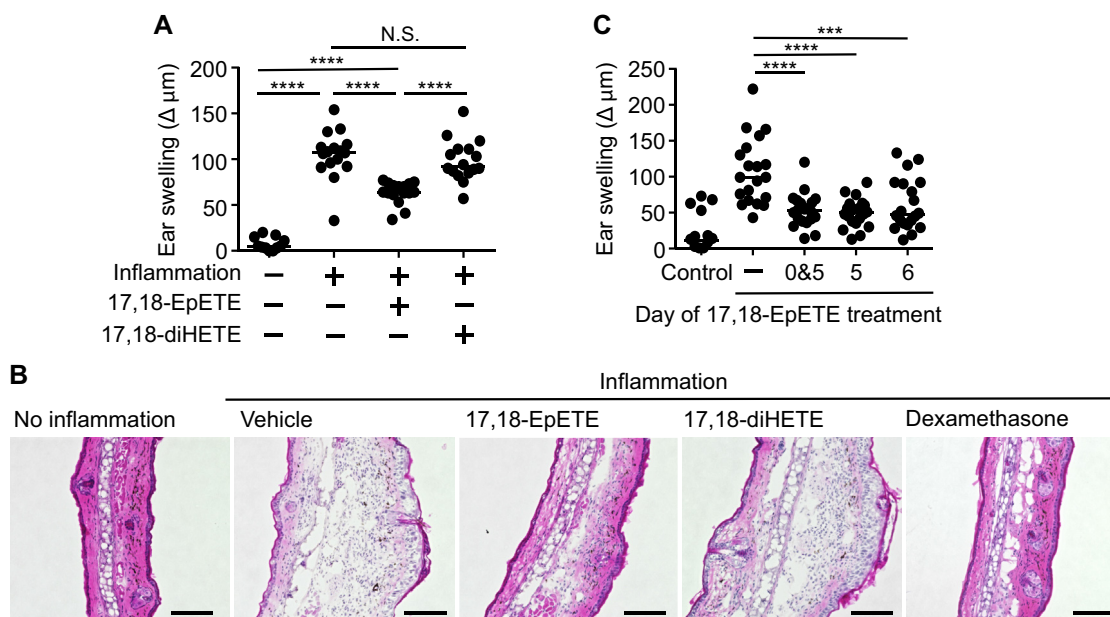


FIG 1. Contact hypersensitivity is ameliorated by 17,18-EpETE but not its metabolite, 17,18-diHETE. **A**, Mice were injected intraperitoneally with either 17,18-EpETE, 17,18-diHETE, or vehicle on days 0 and 5 at 30 minutes before DNFB application. Ear swelling was evaluated on day 7. Data are combined from 3 independent experiments, and each point represents data from individual mice. Center values indicate medians. Statistical significance of differences was evaluated by using 1-way ANOVA. **B**, Frozen ear sections were stained with hematoxylin and eosin and analyzed by means of microscopy. Data are representative of 5 independent experiments. Dexamethasone was applied as a positive control for inhibition of inflammation. Scale bars = 100 μm . **C**, Mice were injected intraperitoneally with either 17,18-EpETE or vehicle on the indicated days at 30 minutes before DNFB application. Ear swelling was evaluated on day 7. Data are combined from 3 independent experiments, and each point represents data from individual mice. Center values indicate medians. Statistical significance of differences was evaluated by means of 1-way ANOVA: *** $P < .001$ and **** $P < .0001$.

release into conditioned medium. Human embryonic kidney 293 (HEK293) cells were transfected with a plasmid encoding alkaline phosphatase–tagged TGF- α with or without a GPR-encoding plasmid.³⁶ Because the TGF- α shedding assay depends on a $G\alpha_q$ - or $G\alpha_{12/13}$ -mediated signaling pathway, some GPRs required coexpression with a $G\alpha$ chimeric protein. Specifically, $G\alpha_{q/13}$ (consisting of the $G\alpha_q$ backbone with C-terminal sequences derived from $G\alpha_{13}$) was coexpressed in HEK293 cells in the assay for GPR84, and $G\alpha_{q/11}$, $G\alpha_{q/13}$, and $G\alpha_{q/6}$ were coexpressed in the assays for GPR41, GPR43, and GPR120, respectively. Transfected HEK293 cells were seeded in serum-free medium in a 96-well plate and stimulated with 17,18-EpETE, 17,18-diHETE, or EPA for 1 hour, followed by addition of para-nitrophenylphosphate (a substrate for alkaline phosphatase) and measurement of para-nitrophenol production at a wavelength of 405 nm.

In vivo imaging

Contact hypersensitivity in mice was induced by using DNFB treatment, as described above; at 12 hours after elicitation, ear skin was observed by using 2-photon excitation microscopy. Neutrophils were visualized by means of intravenous injection of 15 μg of FITC–anti-Ly6G mAb (BioLegend) 2 to 4 hours before imaging. Vessels were visualized by means of intravenous injection of Qtracker 655 (Life Technologies) just before imaging. Neutrophil mobility was monitored for 25 minutes before and after intravenous injection of 25 μg of 17,18-EpETE at the same skin site. The imaging system was composed of a 2-photon microscope (A1-MP; Nikon, Tokyo, Japan) driven by a laser (Chameleon Vision II Ti Sapphire; Coherent, Santa Clara, Calif) tuned to 900 nm and an inverted microscope equipped with a 20 \times objective lens (NA, 0.75; Plan Fluor; Nikon). Fluorescent signals were detected through band-pass emission filters at 525/50 nm (for FITC) and 660/52 nm (for Qtracker 655). Tracking analysis was performed by using Imaris software (Bitplane, Zurich, Switzerland).

Vascular permeability test

The vascular permeability assay was conducted, as reported previously with modification.³⁷ Evans blue dye (1% [wt/vol] solution; Nacalai Tesque) was injected intravenously on day 7, 1 hour before mice were killed. Ears were incubated in 1 mL of 3N KOH (Nacalai Tesque) at 37°C overnight to extract the Evans blue dye. Afterward, the supernatant was added to a tube containing 1 mL of 1.24 mol/L H_3PO_4 and 3 mL of acetone; the contents were mixed by means of vortexing, centrifuged (1280g for 15 minutes at 20°C), and left to phase separate at room temperature for 10 minutes. Absorbance of the aqueous phase (OD_{620}) was measured with the SmartSpec Plus (Bio-Rad Laboratories). The concentration of Evans blue dye was calculated based on a standard curve of known amounts of the dye.

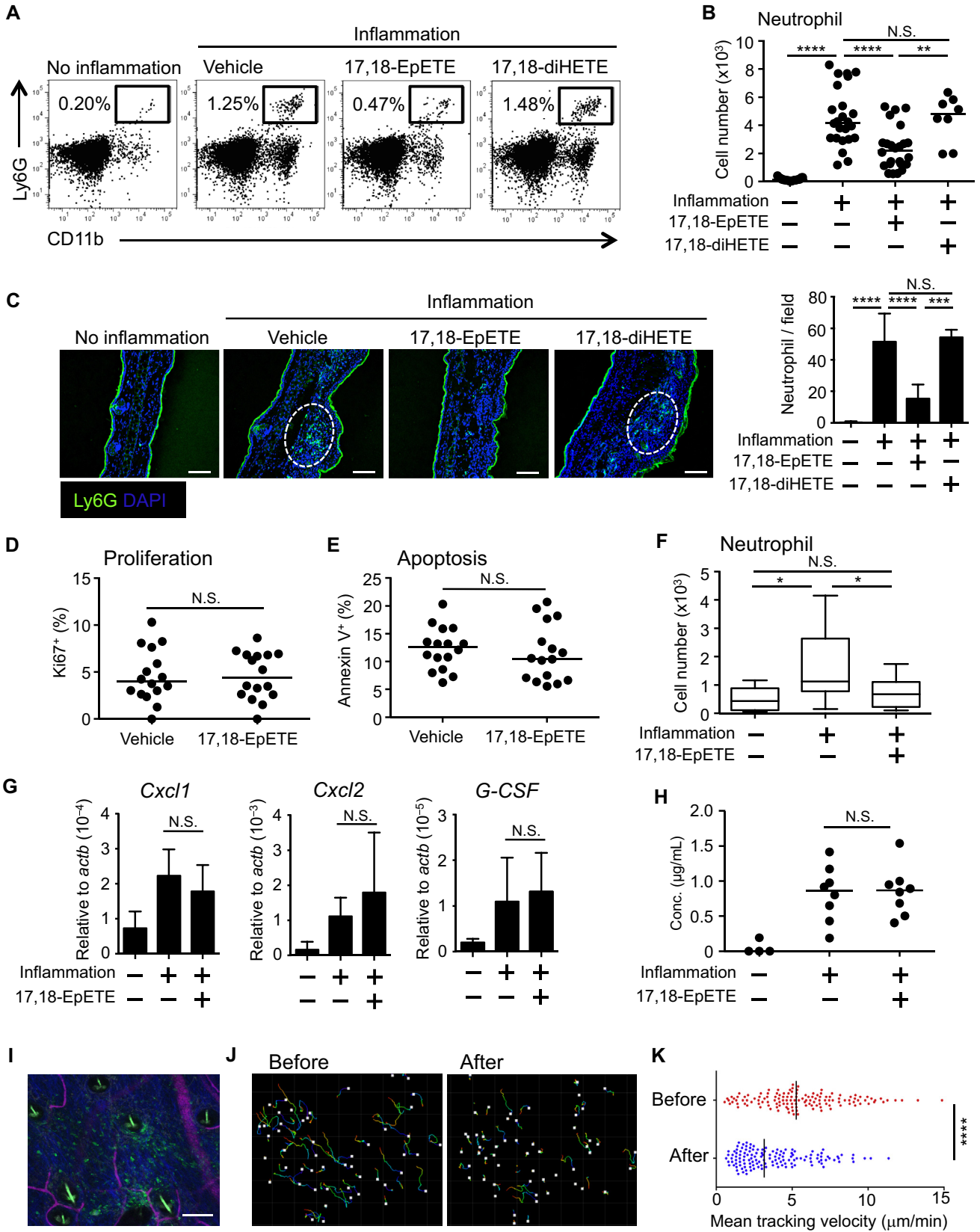
Statistics

Statistical significance was evaluated by using 1-way ANOVA for comparison of multiple groups and the Mann-Whitney test for 2 groups by using Prism 6 software (GraphPad Software, La Jolla, Calif). A P value of less than .05 was considered significant.

RESULTS

17,18-EpETE ameliorates DNFB-induced contact hypersensitivity

To examine the effects of 17,18-EpETE on skin inflammation, we used a murine hapten-induced contact hypersensitivity model. Mice were injected intraperitoneally with 17,18-EpETE or vehicle 30 minutes before stimulation with DNFB as a hapten in the sensitization and elicitation phases of contact



hypersensitivity, which was evaluated by measuring ear thickness (see Fig E1, A, in this article's Online Repository at www.jacionline.org). We first examined ear swelling over time and found that DNFB-induced ear swelling was maximal on day 7 (see Fig E1, B) and that intraperitoneal injection with 17,18-EpETE ameliorated this inflammation (Fig 1, A, and see Fig E1, B). 17,18-EpETE is known to be hydrolyzed by epoxide hydrolase to form 17,18-diHETE.³⁸ Consistent with our previous findings regarding its lack of effect in intestinal allergy,⁹ 17,18-diHETE had little effect on contact hypersensitivity (Fig 1, A). Histologic analysis of ear sections supported the finding that skin inflammation was ameliorated by 17,18-EpETE but not 17,18-diHETE (Fig 1, B). Human patients with eczema have decreased levels of antimicrobial peptides in the skin.³⁹ Consistent with this evidence, various antimicrobial peptides, including cathelicidin, β -defensin 1, and β -defensin 2, showed decreased expression in our DNFB-induced contact hypersensitivity mouse model, and 17,18-EpETE did not influence the expression of these antimicrobial peptides (see Fig E2 in this article's Online Repository at www.jacionline.org).

We next treated mice intraperitoneally with 17,18-EpETE at various time points at both the sensitization and elicitation phases of contact hypersensitivity (days 0 and 5), at the elicitation phase only (day 5), or after elicitation only (day 6). Our results showed that 17,18-EpETE ameliorated ear swelling in all 3 experimental settings (Fig 1, C). Inflammation was ameliorated even when 17,18-EpETE was given only on day 5 or 6, suggesting that 17,18-EpETE suppresses inflammation in the setting of contact hypersensitivity by targeting the elicitation phase (Fig 1, C).

Furthermore, we confirmed that treatment with 17,18-EpETE was effective when it was administered orally or topically to mice (see Fig E3 in this article's Online Repository at www.jacionline.org). Indeed, pharmacokinetic analysis of 17,18-EpETE indicated that a single oral dose of 17,18-EpETE was absorbed into the plasma by 1 to 2 hours after administration (see Fig E4 in this article's Online Repository at www.jacionline.org). Collectively, these findings demonstrate that 17,18-EpETE is an effective lipid metabolite to control contact hypersensitivity both preventively and therapeutically through several administrative routes.

17,18-EpETE does not interfere with iSALT formation, T-cell activation, or macrophage phenotypes

We next examined which types of immune cells were affected by the 17,18-EpETE treatment. A recent study has shown that iSALT formation plays an important role in the elicitation phase of skin inflammation by inducing the activation and proliferation of effector or pathologic T cells.²⁶ Flow cytometric analysis revealed that intraperitoneal treatment with 17,18-EpETE only minimally affected the numbers of DCs and T cells in inflamed skin (see Figs E5 and E6, A, in this article's Online Repository at www.jacionline.org). Indeed, 17,18-EpETE had little effect on the proliferation of T cells (see Fig E6, B). In contrast, topical application of dexamethasone reduced the number of T cells in inflamed skin (see Fig E6, A), suggesting that 17,18-EpETE and dexamethasone exert anti-inflammatory properties through different mechanisms.

FIG 2. 17,18-EpETE inhibits neutrophil mobility and infiltration of the skin. **A-H,** Mice were injected intraperitoneally with either 17,18-EpETE or vehicle on days 0 and 5 at 30 minutes before DNFB application. Ear samples were obtained on day 7. Fig 2, A, Cells were isolated from mouse ears and used for flow cytometric analysis. Numbers indicate the percentage of Ly6G⁺CD11b⁺ neutrophils. Data are representative of 3 independent experiments. Fig 2, B, Numbers of neutrophils were calculated on the basis of total cell numbers and flow cytometric data. Data are combined from 3 independent experiments, and each *point* represents data from individual mice. Center values indicate medians. Statistical significance was evaluated by using 1-way ANOVA: ** $P < .01$ and **** $P < .0001$. *N.S.*, Not significant. Fig 2, C, Ear samples were used for tissue staining. Data are representative of 5 independent experiments. *Dotted circles* indicate the area of neutrophil infiltration. *Scale bars* = 100 μ m. The number of Ly6G⁺ neutrophils per field (magnification $\times 200$) was counted. Data are expressed as means \pm SDs ($n = 4$ -12). Statistical significance was evaluated by using 1-way ANOVA: *** $P < .001$ and **** $P < .0001$. *N.S.*, Not significant. Fig 2, D and E, Expression of Ki67 and Annexin V in Ly6G⁺CD11b⁺ neutrophils was examined by using flow cytometry to assess neutrophil proliferation (Fig 2, D) and survival (Fig 2, E), respectively. Center values indicate medians. Statistical significance was evaluated by using the Mann-Whitney test. *N.S.*, Not significant. Fig 2, F, For *in vivo* labeling of neutrophils, FITC-anti-Ly6G mAb was injected intravenously on day 7 in the contact hypersensitivity model; 30 minutes after injection, cells were isolated from the ears and examined by using flow cytometry. Numbers of FITC⁺ neutrophils were calculated by using total cell numbers and flow cytometric data. Data are combined from 2 independent experiments ($n = 6$ to 12). Center values indicate medians. Statistical significance was evaluated by using 1-way ANOVA: * $P < .05$. *N.S.*, Not significant. Fig 2, G, Ear tissues were homogenized for isolation of mRNA, and quantitative RT-PCR analysis was performed to measure *Cxcl1*, *Cxcl2*, and *G-CSF* expression, which was normalized to that of *Actb*. Data are expressed as means \pm SDs (3 replicate measurements) and representative of 2 independent experiments. Statistical significance was evaluated by using 1-way ANOVA. *N.S.*, Not significant. Fig 2, H, Evans blue solution was injected intravenously at 1 hour before analysis on day 7. The amount of Evans blue dye extracted was measured at OD₆₂₀. Center values indicate medians. Statistical significance was evaluated by using 1-way ANOVA. *N.S.*, Not significant. **I,** Intravital 2-photon imaging of DNFB-induced inflamed skin. Neutrophils and microvasculature were visualized by means of intravenous injection of FITC-anti-Ly6G mAb (green) and Qtracker 655 (far-red), respectively. The blue color indicates collagen fibers. *Scale bar* = 100 μ m. **J,** Imaging analysis of neutrophil mobility in the skin before and after intravenous injection of 17,18-EpETE. *Colored lines* show associated trajectories of the cells. **K,** Summary of mean tracking velocities of neutrophils before and after treatment of mice with 17,18-EpETE. Data points (before treatment, $n = 135$; after treatment, $n = 136$) represent values for individual cells compiled from 3 independent experiments. Center values indicate medians. Statistical significance was evaluated by using the Mann-Whitney test: **** $P < .0001$.

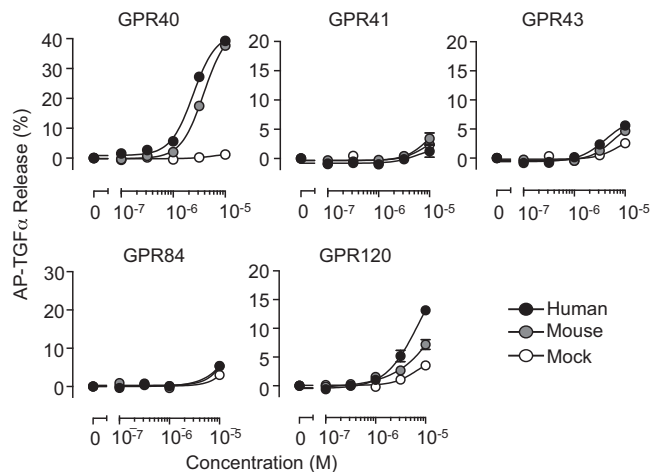


FIG 3. 17,18-EpETE preferentially activates GPR40, weakly activates GPR120, but does not activate GPR41, GPR43, or GPR84. HEK293 cells were transfected with the indicated receptors, and TGF- α shedding assays were performed by using various concentrations of 17,18-EpETE. Data are expressed as means \pm SDs (3-6 replicate measurements) and representative of 2 independent experiments.

We next examined T-cell cytokine production over time, and found that large numbers of IFN- γ -producing T cells were present on day 6, 1 day after elicitation of hypersensitivity (see Fig E6), and further that 17,18-EpETE did not inhibit cytokine production (eg, IFN- γ and IL-17A; see Fig E6, C-E) in inflamed skin. Consistent with those findings, histologic analysis showed that 17,18-EpETE did not inhibit formation of the DC- and T cell-containing iSALT (see Fig E6, F).

In addition to T cells, macrophages play an important role in the development of contact hypersensitivity by inducing iSALT formation.²⁶ In accordance with the findings described above, intraperitoneal treatment with 17,18-EpETE did not alter the number of skin macrophages (see Fig E6, G) or their phenotypes, as judged by expression of *Tnfa* and *Chi3l3* as M1 and M2 markers, respectively (see Fig E6, H). Taken together, these results indicate that 17,18-EpETE has minimal effects on the function of macrophages, DCs, and T cells in the skin.

17,18-EpETE decreases the number of neutrophils by impairing their mobility

Given that depletion of neutrophils prevents development of inflammation,^{20,22,23} neutrophils play a crucial role in induction of contact hypersensitivity. Neutrophils express FasL and perforin, which play important roles in the development of contact hypersensitivity⁴⁰; however, intraperitoneal treatment with 17,18-EpETE did not alter expression levels of these factors (see Fig E7 in this article's Online Repository at www.jacionline.org). In contrast, compared with untreated mice with contact hypersensitivity, those given intraperitoneal treatment with 17,18-EpETE had fewer neutrophils in the skin (Fig 2, A and B). Consistent with our findings regarding ear swelling in mice (Fig 1), 17,18-diHETE did not influence skin neutrophil numbers (Fig 2, A and B). Indeed, histologic analysis showed a reduction in numbers of Ly6G⁺ neutrophils in the skin of 17,18-EpETE- but not 17,18-diHETE-treated mice (Fig 2, C).

We then hypothesized that 17,18-EpETE might reduce neutrophil numbers in the skin by modulating either (1) neutrophil

proliferation, (2) neutrophil survival, or (3) infiltration of neutrophils into the skin. To test the effect of 17,18-EpETE on the proliferation and survival of neutrophils, we stained neutrophils with Ki67 and Annexin V, respectively. Flow cytometric analysis revealed that 17,18-EpETE did not alter neutrophil proliferation (Fig 2, D) or the percentage of Annexin V⁺ apoptotic neutrophils (Fig 2, E) in the skin. These findings exclude 2 possibilities regarding the effect of 17,18-EpETE on the proliferation and survival of neutrophils in the skin.

To address the possibility that 17,18-EpETE affects neutrophil infiltration into the skin, we used an *in vivo* labeling system based on FITC-conjugated anti-Ly6G mAb.^{32,33} Infiltration of FITC-labeled neutrophils was detected in the skin of mock-treated mice after induction of contact hypersensitivity, but their numbers were significantly decreased in the skin of 17,18-EpETE-treated mice (Fig 2, F). This finding showed that 17,18-EpETE treatment inhibited infiltration of neutrophils from the blood circulation into the skin of mice with contact hypersensitivity. Although CXCL1, CXCL2, and G-CSF are known to be neutrophil-recruiting chemokines and cytokines,^{19,20} intraperitoneal injection of 17,18-EpETE did not affect their gene expression in inflamed skin (Fig 2, G). In addition, the amount of G-CSF protein in serum was unchanged by intraperitoneal injection of 17,18-EpETE (see Fig E8 in this article's Online Repository at www.jacionline.org). Furthermore, intraperitoneal injection of 17,18-EpETE had no effect on vascular permeability (Fig 2, H).

We then used intravital 2-photon microscopy to examine *in vivo* neutrophil mobility in the skin of mice with contact hypersensitivity (Fig 2, I). This analysis revealed that neutrophil mobility in the skin was impaired after intravenous treatment with 17,18-EpETE (Fig 2, J and K, and see Videos E1 and E2 in this article's Online Repository at www.jacionline.org). These findings together suggest that 17,18-EpETE directly regulates neutrophil mobility without affecting chemokine expression or vascular permeability.

17,18-EpETE acts through GPR40 to control neutrophil-mediated contact hypersensitivity

We next aimed to elucidate the molecular mechanism underlying the anti-inflammatory properties of 17,18-EpETE. The anti-inflammatory effect of 17,18-EpETE reportedly is mediated by PPAR- γ ,¹⁰ but unlike rosiglitazone, a PPAR- γ agonist, 17,18-EpETE only weakly activated PPAR- γ (unpublished data). Therefore we conducted TGF- α shedding assays to identify the GPR for 17,18-EpETE.³⁶ Among several types of GPRs, 17,18-EpETE strongly activated GPR40, weakly activated GPR120, and did not activate GPR41, GPR43, or GPR84 (Fig 3). Although EPA is recognized by GPR40,¹⁵ its activation activity was much weaker than that of 17,18-EpETE (Fig 4, A). In addition, 17,18-diHETE did not activate GPR40 (Fig 4, A), which is consistent with its lack of anti-inflammatory activity (Fig 1, A and B). Therefore 17,18-EpETE is a unique lipid metabolite in that it is a strong agonist of GPR40.

These findings led us to examine whether the anti-inflammatory effects of 17,18-EpETE depend on GPR40. To address this issue, we treated mice intraperitoneally with GW1100, a GPR40 antagonist, at 30 minutes before intraperitoneal administration of 17,18-EpETE in the DNFB-induced contact hypersensitivity model. We found that treatment

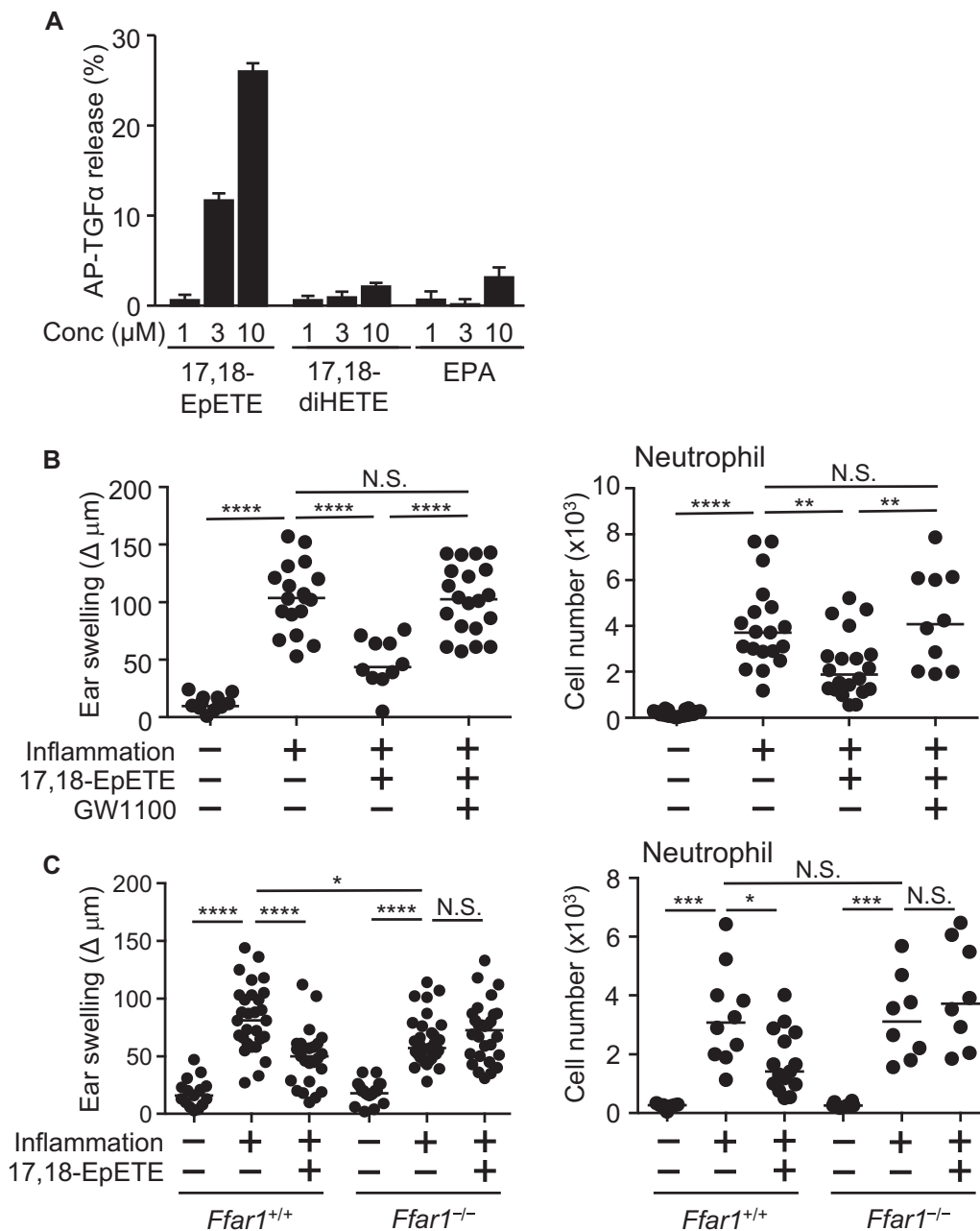


FIG 4. 17,18-EpETE acts through GPR40 to control neutrophil-mediated contact hypersensitivity. **A**, The TGF- α shedding assay was performed to examine the reactivity of GPR40-expressing cells to various concentrations of 17,18-EpETE, 17,18-diHETE, and EPA. Data are expressed as means \pm SDs (3-6 replicate measurements) and representative of 2 independent experiments. **B**, At both the sensitization and elicitation phases, mice were injected intraperitoneally with either GW1100 or vehicle 30 minutes before intraperitoneal 17,18-EpETE injection; mice were then stimulated with DNFB at 30 minutes after intraperitoneal 17,18-EpETE injection. Ear swelling (*left*) and numbers of Ly6G⁺CD11b⁺ neutrophils (*right*) were evaluated on day 7. Data are combined from 3 independent experiments, and each *point* represents data from an individual mouse. Center values indicate medians. Statistical significance was evaluated by using 1-way ANOVA: ** P < .01 and **** P < .0001. *N.S.*, Not significant. **C**, *Ffar1*^{+/+} mice and *Ffar1*^{-/-} mice were injected intraperitoneally with either 17,18-EpETE or vehicle at 30 minutes before DNFB treatment at both the sensitization and elicitation phases. Ear swelling (*left*) and numbers of Ly6G⁺CD11b⁺ neutrophils (*right*) were evaluated on day 7. Data are combined from 3 independent experiments, and each *point* represents data from an individual mouse. Center values indicate medians. Statistical significance was evaluated by using 1-way ANOVA: * P < .05, *** P < .001, and **** P < .0001. *N.S.*, Not significant.

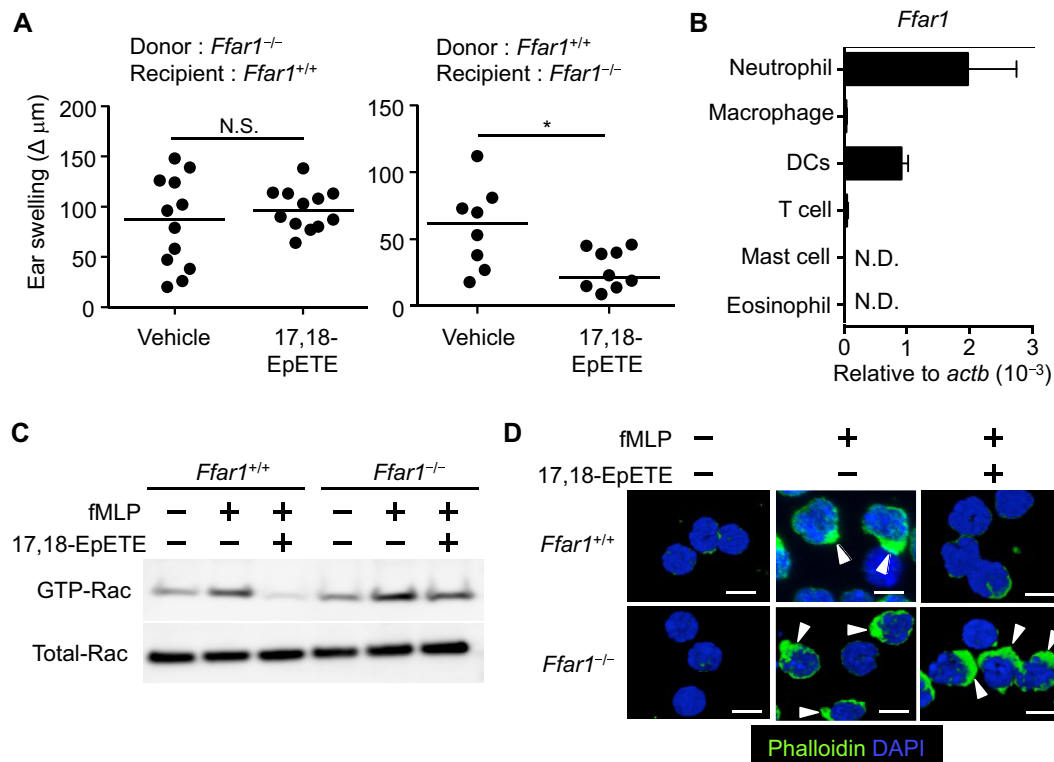


FIG 5. GPR40 expressed on neutrophils plays a pivotal role in the control of neutrophil trafficking in the setting of contact hypersensitivity. **A**, Bone marrow transplantation was conducted to evaluate the requirement of GPR40 on hematopoietic or nonhematopoietic cells for inhibition of contact hypersensitivity by 17,18-EpETE. Contact hypersensitivity was induced by DNFB in bone marrow chimera mice, and ear swelling was evaluated on day 7. Mice were injected intraperitoneally with either 17,18-EpETE or vehicle on days 0 and 5 at 30 minutes before DNFB application. Data are combined from 3 independent experiments, and each *point* represents data from an individual mouse. Center values indicate medians. Statistical significance was evaluated by using the Mann-Whitney test: * $P < .05$. N.S., Not significant. **B**, CD45⁺Gr1^{high}CD11b⁺ neutrophils, CD45⁺Gr1^{low}CD11b⁺ macrophages, CD45⁺F4/80⁻CD11c⁺ DCs, CD45⁺CD3e⁺ T cells, CD45⁺c-Kit⁺FcεRI⁺ mast cells, and CD45⁺Siglec-F⁺CD11b⁺ eosinophils were isolated from DNFB-stimulated ears, and quantitative RT-PCR analysis was performed to analyze gene expression of *Ffar1*. Data are expressed as means \pm SEMs (3 replicate measurements) and representative of 2 independent experiments. N.D., Not determined. **C**, Immunoblot analysis for GTP-bound and total Rac in bone marrow–derived neutrophils isolated from *Ffar1*^{+/+} or *Ffar1*^{-/-} mice. Neutrophils were treated with either 17,18-EpETE or vehicle *in vitro* 15 minutes before stimulation with fMLP. Similar results were obtained from 3 independent experiments. **D**, Pseudopod formation was evaluated by staining neutrophils with phalloidin. Neutrophils were treated with either 17,18-EpETE or vehicle *in vitro* 15 minutes before stimulation with fMLP. Data are representative of 3 independent experiments. Arrows indicate pseudopod structures. Scale bars = 5 μm .

with GW1100 abolished the inhibitory effect of 17,18-EpETE. Indeed, mice that received both 17,18-EpETE and GW1100 had inflammatory symptoms (ie, ear swelling and neutrophil infiltration; Fig 4, B). To further confirm the involvement of GPR40 in the 17,18-EpETE–mediated inhibitory activity, we used mice lacking GPR40 (*Ffar1*^{-/-} mice).¹⁶ As expected, 17,18-EpETE had little effect on ear swelling and neutrophil numbers in the skin of *Ffar1*^{-/-} mice (Fig 4, C). Given that GPR40 expression exerts anti-inflammatory effects, we expected that fasiglifam (TAK-875), an agonist of GPR40,⁴¹ would lead to an anti-inflammatory response as well. However, in contrast to 17,18-EpETE, TAK-875 did not inhibit ear swelling (see Fig E9 in this article's Online Repository at www.jacionline.org).

Pivotal roles of GPR40 in the control of neutrophil trafficking

A previous study showed that GPR40 is expressed in the skin.⁴² To address whether hematopoietic cells, nonhematopoietic cells,

or both are required for the GPR40-mediated inhibition of contact hypersensitivity, we used wild-type and *Ffar1*^{-/-} mice to generate bone marrow chimeras. Irradiated wild-type mice that received *Ffar1*^{-/-} bone marrow cells had contact hypersensitivity even after intraperitoneal injection with 17,18-EpETE (Fig 5, A). In contrast, irradiated *Ffar1*^{-/-} mice given wild-type bone marrow cells showed inhibition of contact hypersensitivity after intraperitoneal injection with 17,18-EpETE (Fig 5, A). Although GPR40 is expressed reportedly on nonhematopoietic cells, such as keratinocytes,⁴² our results indicate that GPR40 expression on hematopoietic cells is required to exert the anti-inflammatory properties of 17,18-EpETE.

We next examined which hematopoietic cells expressed GPR40 in the inflammatory skin tissue and thus were responsible for the specific reactivity to 17,18-EpETE. We purified several populations of hematopoietic cells with increased numbers in inflamed skin and found that GPR40 expression was absent or negligible in T cells, macrophages, mast cells, and eosinophils but that neutrophils and DCs (Fig 5, B) and splenic B cells expressed

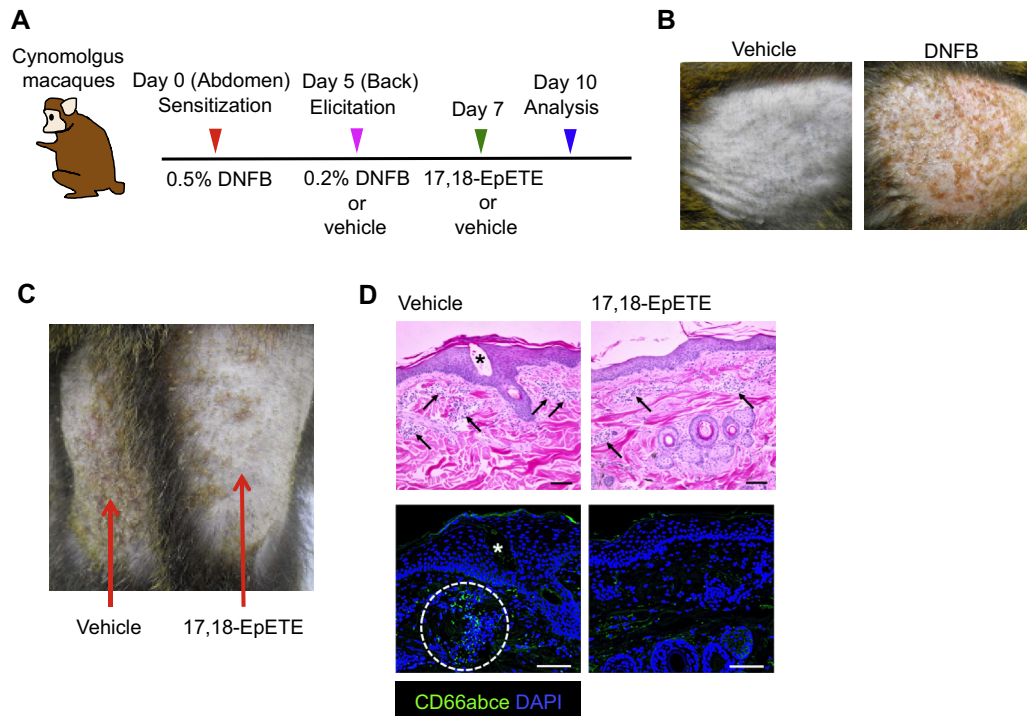


FIG 6. Therapeutic treatment with 17,18-EpETE ameliorates DNFB-induced contact hypersensitivity in cynomolgus macaques. **A**, Experimental protocol for induction of contact hypersensitivity by DNFB in a cynomolgus macaque and its treatment with 17,18-EpETE. **B**, Cynomolgus macaques treated with DNFB on days 0 and 5 had reddening and eczema of their back skin on day 7. **C**, Representative photographs of the back skin obtained 3 days after the topical application of 17,18-EpETE (right side) or vehicle (left side). **D**, Skin biopsy samples were embedded in paraffin blocks, and resulting sections were analyzed by means of hematoxylin and eosin staining (top) and staining with anti-CD66abce mAb (green) and DAPI (blue; bottom). Data are representative of 2 independent experiments (n = 3). Asterisks denote vesicle formation, and arrows indicate cell infiltration. The dotted circle delineates the area of neutrophil infiltration.

GPR40 (see Fig E10, A, in this article's Online Repository at www.jacionline.org). Despite expression of GPR40, numbers of DCs and B cells in inflamed skin (see Figs E5 and E10, B) and the amount of serum IgM antibody (see Fig E10, C) were unchanged by intraperitoneal injection of 17,18-EpETE. Because DCs regulate neutrophil migration through production of IL-10 and CXCL8,^{43,44} we examined the expression of these genes in inflamed ear tissue. We found that 17,18-EpETE did not affect the expression of *Il10*, *Cxcl1*, or *Cxcl2* (mouse homologue of human *Cxcl8*; Fig 2, G, and see Fig E11 in this article's Online Repository at www.jacionline.org), thus suggesting that 17,18-EpETE exerts its inhibitory effects directly on neutrophils.

We next examined the molecular mechanisms of direct effects of 17,18-EpETE on neutrophils. Neutrophils purified from bone marrow were stimulated with fMLP, a bacteria-derived neutrophil chemoattractant,⁴⁵ in the absence or presence of 17,18-EpETE *in vitro*. As previously reported,⁴⁶ the treatment of neutrophils with fMLP induced Rac activation, a crucial process for cell trafficking (Fig 5, C). The fMLP-induced Rac activation was inhibited when neutrophils isolated from wild-type, but not *Ffar1*^{-/-}, mice were treated with 17,18-EpETE (Fig 5, C). Monomeric globular actin polymerizes to form filamentous actin (F-actin) on Rac activation at the leading edge of the cell movement, the structure of F-actin accumulation is known as a pseudopod.⁴⁷ Indeed, 17,18-EpETE treatment blocked fMLP-induced pseudopod formation in wild-type neutrophils (Fig 5, D). Furthermore, we found that 17,18-EpETE had little

effect on pseudopod formation in *Ffar1*^{-/-} neutrophils (Fig 5, D). In contrast, 17,18-EpETE did not affect wild-type neutrophils on the cell surface expression of CD18 and CXCR2, receptors for adhesion molecules (eg, ICAM1) and chemokines (eg, CXCL1 and CXCL2), both of which play important roles in neutrophil infiltration to the skin (see Fig E12 in this article's Online Repository at www.jacionline.org).^{48,49}

These results show that 17,18-EpETE inhibits neutrophil infiltration into the skin through activation of GPR40-mediated signals, thereby inhibiting Rac activation and blocking pseudopod formation in neutrophils.

17,18-EpETE ameliorates contact hypersensitivity in cynomolgus macaques

Using the TGF- α shedding assay, we found that 17,18-EpETE activated not only murine GPR40 but also the human form (Fig 3), prompting us to examine whether the inhibitory function of 17,18-EpETE is effective in control of skin inflammation in cynomolgus macaques. Because cynomolgus macaques are a useful animal model for allergic diseases,⁵⁰ we first confirmed that, as in the murine model, the treatment of cynomolgus macaques with DNFB at days 0 and 5 led to the development of skin inflammation with eczema formation on day 7 (Fig 6, A and B). We then topically applied 17,18-EpETE and vehicle to separate areas of the back skin on day 7 and monitored the progression of skin inflammation until day 10. We found that

topical application of 17,18-EpETE ameliorated skin inflammation in cynomolgus macaques. Indeed, skin reddening and eczema were decreased in the 17,18-EpETE-treated area, whereas these symptoms persisted in the vehicle application area (Fig 6, C). Histologic analysis showed that topical application of 17,18-EpETE reduced eczema-associated vesicle formation in cynomolgus macaques (Fig 6, D), and immunohistologic analysis revealed that 17,18-EpETE application decreased the numbers of CD66abce⁺ neutrophils in the skin (Fig 6, D). These findings suggest collectively that 17,18-EpETE is an effective compound for topical therapy of allergic skin inflammation in cynomolgus macaques.

DISCUSSION

In this study we showed that 17,18-EpETE acts as a GPR40 ligand and achieves its antiallergic and anti-inflammatory effects by inhibiting neutrophil mobility in both murine and cynomolgus macaque models of contact hypersensitivity.

GPR40 was expressed in neutrophils and DCs in inflamed skin and in splenic B cells. In contrast to its critical role on GPR40 and thus in decreasing neutrophil mobility, 17,18-EpETE had a negligible effect on DCs and B cells. A previous study suggested that GPR40-mediated signaling in keratinocytes is involved in inhibition of contact hypersensitivity and that topical treatment with GW9508, an agonist of GPR40 and GPR120, inhibited the development of contact hypersensitivity in mice by suppressing production of CXCL10, a T-cell attractant.⁴² However, our bone marrow chimera analysis showed that GPR40 expression on hematopoietic cells rather than nonhematopoietic cells played an important role in the control of contact hypersensitivity by 17,18-EpETE. Furthermore, we found that TAK-875, a GPR40 agonist, was ineffective in the treatment of contact hypersensitivity. Given that GPR40-mediated signaling pathways, such as Gα_q and Gα_s, are dependent on ligand types⁵¹ and that Gα-mediated signaling pathways differ in distinct cell subsets,⁵² we suppose that 17,18-EpETE targets specific GPR40-mediated signaling to impair neutrophil mobility without affecting the functions of DCs, B cells, and keratinocytes.

Of note, ear swelling was decreased in *Ffar1*^{-/-} mice in comparison with *Ffar1*^{+/+} mice in the setting of DNFB-induced contact hypersensitivity, suggesting that GPR40 positively regulates the development of inflammation. However, ear swelling was unchanged in mice treated with GW1100, a GPR40 antagonist. In addition, neutrophil functions, such as Rac activation and pseudopod formation, were induced normally by fMLP in *Ffar1*^{-/-} mice. Therefore our findings show that the 17,18-EpETE-mediated impairment of neutrophil mobility is dependent on the GPR40 receptor. Although adhesion molecules (ICAM1-CD18), chemokines (CXCL1/CXCL2-CXCR2), and a cytokine (G-CSF) are known targets for the control of neutrophil infiltration into the skin and the development of contact hypersensitivity,^{20,48,49} their expression remained unchanged after treatment with 17,18-EpETE. In contrast, 17,18-EpETE prevented Rac activation through GPR40-mediated signaling in neutrophils. Rac belongs to the Rho GTPase family, and its conversion from its GDP form to the GTP form plays a crucial role in cell migration because it enables Rac to interact with scaffold protein, lamellipodin, and consequently inducing actin filament extension.⁵³

GPR40-mediated signals potentially could be modulated by either Gα_i, Gα_s, or Gα_q^{42,51}; Gα_i and Gα_s inhibit and promote cytosolic cyclic AMP accumulation, respectively, whereas Gα_q increases the cytosolic Ca²⁺ level. Therefore in 17,18-EpETE-treated neutrophils GPR40-mediated signals likely modulate the activities of protein kinases A and C, which are regulated by cytosolic cyclic AMP and Ca²⁺ levels, respectively. In addition, P-Rex1 functions as a major guanine-nucleotide-exchange factor for Rac in fMLP stimulation, and the activity of P-Rex1 is known to be inhibited by protein kinase A or enhanced by protein kinase C.⁵⁴

It is noteworthy that GPR40-mediated signaling pathways are dependent on ligand types. Indeed, ALA and DHA induce only Gα_q-mediated signals through GPR40, whereas the synthetic GPR40 agonist AM-1638 and AM-5262 induce both Gα_q- and Gα_s-mediated signals.⁵¹ In addition, Gα_q plus Gα_s dual agonists appeared to induce incretin secretion more efficiently than did a Gα_q single-targeting agonist.⁵¹ It remains to be investigated which Gα protein(s) are stimulated by 17,18-EpETE, but our current findings imply that the 17,18-EpETE-GPR40 axis is likely to signal through Gα_s-mediated pathways, which lead to activation of protein kinase A and consequent inhibition of the guanine-nucleotide-exchange factor for Rac activity of P-Rex1.

We found that 17,18-EpETE ameliorated contact hypersensitivity not only preventively but also therapeutically. After their infiltration into an inflammatory site, neutrophils produce chemical mediators, such as myeloperoxidase and CXCL10.^{55,56} Reportedly, Rac activation is required for neutrophil degranulation,⁵⁷ suggesting that 17,18-EpETE might prevent neutrophil degranulation and cell mobility. Furthermore, expression of FasL and perforin by neutrophils is required for the development of contact hypersensitivity.⁴⁰ Therefore, in addition to inhibiting neutrophil trafficking into the skin, therapeutic treatment of 17,18-EpETE can exert antiallergy and anti-inflammatory properties by inhibiting the degranulation of neutrophils (eg, by affecting perforin and myeloperoxidases) or their expression of cytotoxic molecules (eg, FasL and perforin). However, our analysis indicated that 17,18-EpETE treatment had no effect on expression of FasL and perforin in neutrophils, suggesting that the control of neutrophil infiltration is the primary biological target of 17,18-EpETE.

Our current study shows that a strong GPR40 ligand ability and the antiallergic and anti-inflammatory properties of 17,18-EpETE require its epoxy structure. Indeed, 17,18-diHETE exerts neither GPR40 signals nor antiallergic inflammatory properties. Conversion from 17,18-EpETE into 17,18-diHETE is mediated by soluble epoxide hydrolase; reportedly, inhibition of epoxide hydrolase ameliorates inflammatory responses, such as hypertension, diabetes, and pain pathways, thus providing organ protection in models of cardiac, renal, and brain injury.⁵⁸ In addition, conversion of EPA into 17,18-EpETE is another key step for its antiallergy and anti-inflammatory effects. 17,18-EpETE is converted from EPA by CYP. It is known that CYPs has polymorphisms.⁵⁹ In addition, among the CYP subfamily, CYP1A, CYP2C, and CYP2J can synthesize 17,18-EpETE from EPA.⁶⁰⁻⁶² Therefore the generation and conversion of 17,18-EpETE appear to be critical determinants in the control of allergic and inflammatory diseases.

17,18-EpETE ameliorated contact hypersensitivity in mice and cynomolgus macaques by inhibiting neutrophil mobility.

Neutrophils are known to play key roles in other forms of dermatitis, such as atopic dermatitis and psoriasis,^{63,64} implicating the effectiveness of 17,18-EpETE to control of various kinds of dermatitis. In addition, our previous work showed that 17,18-EpETE inhibited the development of type I allergic responses by suppressing mast cell degranulation.⁹ Because mast cells do not express GPR40, another cell population was likely responsible for the antiallergic properties of 17,18-EpETE in the intestine. Regarding this issue, GPR40-mediated signaling is reported to enhance the intestinal epithelial barrier.⁶⁵ Because intestinal allergy is associated with a “leaky gut,”⁶⁶ it is plausible that 17,18-EpETE treatment inhibits mast cell degranulation by decreasing allergen entry into the body. These findings suggest collectively that 17,18-EpETE is a prospective compound for the prevention and treatment of various types of allergy and inflammation in several tissues.

A compound’s route of administration is an important factor in its clinical utility. In this sense 17,18-EpETE is clinically attractive because it is effective not only through systemic injection but also through oral and topical application. Therefore 17,18-EpETE might act on circulating neutrophils, as well as those in skin lesions, after delivery to the tissue from the bloodstream.

We also found that the anti-inflammatory activity of dexamethasone was stronger than that of 17,18-EpETE, presumably because of dexamethasone’s additional effect on T cells. Because a reduction in T-cell numbers can increase the risk of infectious diseases, we might reserve the use of steroids for cases of severe inflammation and then, once the severity has decreased, change to 17,18-EpETE, which had few effects on T-cell function.

In addition, we recently reported that the EPA-derived ω 3 lipid mediator resolvin E1 inhibited DC trafficking in the setting of contact hypersensitivity.²⁸ Indeed, resolvin E1 inhibited both the sensitization and elicitation phases, including iSALT formation and subsequent DC-induced inflammatory cytokine production (eg, IFN- γ) from T cells. The different effects of resolvin E1 and 17,18-EpETE probably reflect the different receptors targeted. Resolvin E1 is a partial agonist of BLT1⁶⁷ and inhibited the development of contact hypersensitivity through attenuation of leukotriene B₄-BLT1 signaling in DCs.²⁸ In contrast, 17,18-EpETE activated GPR40-mediated signals in neutrophils to inhibit their mobility. Our preliminary experiments indicated that a mixture of 17,18-EpETE and resolvin E1 decreased the numbers of DCs and IFN- γ -producing T cells, as well as neutrophil counts, in inflamed skin (unpublished data). Thus 17,18-EpETE and resolvin E1 can exert synergic anti-inflammatory effects on skin inflammation.

Therefore EPA-derived ω 3 lipid mediators (ie, 17,18-EpETE and resolvin E1) exert their antiallergy and anti-inflammatory properties in the setting of contact hypersensitivity by targeting different immune cell populations (eg, neutrophils and DCs) that express different receptors (eg, GPR40 and BLT1), thus providing a new therapeutic strategy through combined use of both lipid mediators.

We thank Drs Ken Ishii, Takuya Yamamoto, and Mayuri Tanaka (NIBIOHN) and Drs Makoto Murakami and Yoshitaka Taketomi (Tokyo Metropolitan Institute of Medical Science, Tokyo, Japan) for helpful discussion and technical advice. We also thank our laboratory members for helpful discussion.

Key messages

- Contact hypersensitivity is ameliorated by 17,18-EpETE, a lipid metabolite of EPA.
- 17,18-EpETE activates GPR40 on neutrophils and inhibits their infiltration to the site of inflammation.

REFERENCES

1. Jangale NM, Devarshi PP, Dubal AA, Ghule AE, Koppikar SJ, Bodhankar SL, et al. Dietary flaxseed oil and fish oil modulates expression of antioxidant and inflammatory genes with alleviation of protein glycation status and inflammation in liver of streptozotocin-nicotinamide induced diabetic rats. *Food Chem* 2013;141:187-95.
2. Chang HH, Chen CS, Lin JY. Dietary perilla oil inhibits proinflammatory cytokine production in the bronchoalveolar lavage fluid of ovalbumin-challenged mice. *Lipids* 2008;43:499-506.
3. Hansen S, Strom M, Maslova E, Dahl R, Hoffmann HJ, Rytter D, et al. Fish oil supplementation during pregnancy and allergic respiratory disease in the adult offspring. *J Allergy Clin Immunol* 2017;139:104-11.e4.
4. Brick T, Schober Y, Bocking C, Pekkanen J, Genuneit J, Loss G, et al. ω -3 fatty acids contribute to the asthma-protective effect of unprocessed cow’s milk. *J Allergy Clin Immunol* 2016;137:1699-706.e13.
5. Magnusson J, Kull I, Westman M, Hakansson N, Wolk A, Melen E, et al. Fish and polyunsaturated fat intake and development of allergic and nonallergic rhinitis. *J Allergy Clin Immunol* 2015;136:1247-53, e1-2.
6. Serhan CN. Pro-resolving lipid mediators are leads for resolution physiology. *Nature* 2014;510:92-101.
7. Miyata J, Arita M. Role of ω -3 fatty acids and their metabolites in asthma and allergic diseases. *Allergol Int* 2015;64:27-34.
8. Zhang MJ, Spite M. Resolvins: anti-inflammatory and proresolving mediators derived from ω -3 polyunsaturated fatty acids. *Annu Rev Nutr* 2012;32:203-27.
9. Kunisawa J, Arita M, Hayasaka T, Harada T, Iwamoto R, Nagasawa R, et al. Dietary ω 3 fatty acid exerts anti-allergic effect through the conversion to 17,18-epoxyeicosatetraenoic acid in the gut. *Sci Rep* 2015;5:9750.
10. Morin C, Sirois M, Echave V, Albadine R, Rousseau E. 17,18-epoxyeicosatetraenoic acid targets PPAR γ and p38 mitogen-activated protein kinase to mediate its anti-inflammatory effects in the lung: role of soluble epoxide hydrolase. *Am J Respir Cell Mol Biol* 2010;43:564-75.
11. Yanai R, Mulki L, Hasegawa E, Takeuchi K, Sweigard H, Suzuki J, et al. Cytochrome P450-generated metabolites derived from ω -3 fatty acids attenuate neovascularization. *Proc Natl Acad Sci U S A* 2014;111:9603-8.
12. Kubota T, Arita M, Isobe Y, Iwamoto R, Goto T, Yoshioka T, et al. Eicosapentaenoic acid is converted via ω -3 epoxygenation to the anti-inflammatory metabolite 12-hydroxy-17,18-epoxyeicosatetraenoic acid. *FASEB J* 2014;28:586-93.
13. Brown AJ, Goldsworthy SM, Barnes AA, Eilert MM, Tcheang L, Daniels D, et al. The orphan G protein-coupled receptors GPR41 and GPR43 are activated by propionate and other short chain carboxylic acids. *J Biol Chem* 2003;278:11312-9.
14. Wang J, Wu X, Simonavicius N, Tian H, Ling L. Medium-chain fatty acids as ligands for orphan G protein-coupled receptor GPR84. *J Biol Chem* 2006;281:34457-64.
15. Yan Y, Jiang W, Spinetti T, Tardivel A, Castillo R, Bourquin C, et al. ω -3 fatty acids prevent inflammation and metabolic disorder through inhibition of NLRP3 inflammasome activation. *Immunity* 2013;38:1154-63.
16. Steneberg P, Rubins N, Bartoov-Shifman R, Walker MD, Edlund H. The FFA receptor GPR40 links hyperinsulinemia, hepatic steatosis, and impaired glucose homeostasis in mouse. *Cell Metab* 2005;1:245-58.
17. Weidinger S, Novak N. Atopic dermatitis. *Lancet* 2016;387:1109-22.
18. Peiser M, Tralau T, Heidler J, Api AM, Arts JH, Basketter DA, et al. Allergic contact dermatitis: epidemiology, molecular mechanisms, in vitro methods and regulatory aspects. Current knowledge assembled at an international workshop at BfR, Germany. *Cell Mol Life Sci* 2012;69:763-81.
19. Honda T, Egawa G, Grabbe S, Kabashima K. Update of immune events in the murine contact hypersensitivity model: toward the understanding of allergic contact dermatitis. *J Invest Dermatol* 2013;133:303-15.
20. Christensen AD, Skov S, Haase C. The role of neutrophils and G-CSF in DNFB-induced contact hypersensitivity in mice. *Immun Inflamm Dis* 2014;2:21-34.
21. Tsuji RF, Szczepanik M, Kawikova I, Paliwal V, Campos RA, Itakura A, et al. B cell-dependent T cell responses: IgM antibodies are required to elicit contact sensitivity. *J Exp Med* 2002;196:1277-90.

22. Weber FC, Nemeth T, Csepregi JZ, Dudeck A, Roers A, Ozsvári B, et al. Neutrophils are required for both the sensitization and elicitation phase of contact hypersensitivity. *J Exp Med* 2015;212:15-22.
23. Moniaga CS, Watanabe S, Honda T, Nielsen S, Hara-Chikuma M. Aquaporin-9-expressing neutrophils are required for the establishment of contact hypersensitivity. *Sci Rep* 2015;5:15319.
24. Mori T, Kabashima K, Yoshiki R, Sugita K, Shiraiishi N, Onoue A, et al. Cutaneous hypersensitivities to hapten are controlled by IFN- γ -upregulated keratinocyte Th1 chemokines and IFN- γ -downregulated langerhans cell Th2 chemokines. *J Invest Dermatol* 2008;128:1719-27.
25. Nakae S, Komiyama Y, Nambu A, Sudo K, Iwase M, Homma I, et al. Antigen-specific T cell sensitization is impaired in IL-17-deficient mice, causing suppression of allergic cellular and humoral responses. *Immunity* 2002;17:375-87.
26. Natsuaki Y, Egawa G, Nakamizo S, Ono S, Hanakawa S, Okada T, et al. Perivascular leukocyte clusters are essential for efficient activation of effector T cells in the skin. *Nat Immunol* 2014;15:1064-9.
27. Kim TH, Kim GD, Jin YH, Park YS, Park CS. ω -3 fatty acid-derived mediator, Resolvin E1, ameliorates 2,4-dinitrofluorobenzene-induced atopic dermatitis in NC/Nga mice. *Int Immunopharmacol* 2012;14:384-91.
28. Sawada Y, Honda T, Hanakawa S, Nakamizo S, Murata T, Ueharaguchi-Tanada Y, et al. Resolvin E1 inhibits dendritic cell migration in the skin and attenuates contact hypersensitivity responses. *J Exp Med* 2015;212:1921-30.
29. Honjo S. The Japanese Tsukuba Primate Center for Medical Science (TPC): an outline. *J Med Primatol* 1985;14:75-89.
30. Mizuno K, Morizane S, Takiguchi T, Iwatsuki K. Dexamethasone but not tacrolimus suppresses TNF- α -induced thymic stromal lymphopoietin expression in lesional keratinocytes of atopic dermatitis model. *J Dermatol Sci* 2015;80:45-53.
31. Nagatake T, Fukuyama S, Sato S, Okura H, Tachibana M, Taniuchi I, et al. Central role of core binding factor β 2 in mucosa-associated lymphoid tissue organogenesis in mouse. *PLoS One* 2015;10:e0127460.
32. Zachariah MA, Cyster JG. Neural crest-derived pericytes promote egress of mature thymocytes at the corticomedullary junction. *Science* 2010;328:1129-35.
33. Nitta T, Hata M, Gotoh S, Seo Y, Sasaki H, Hashimoto N, et al. Size-selective loosening of the blood-brain barrier in claudin-5-deficient mice. *J Cell Biol* 2003;161:653-60.
34. Morrison AR, Yarovsky TO, Young BD, Moraes F, Ross TD, Ceneri N, et al. Chemokine-coupled β 2 integrin-induced macrophage Rac2-Myosin IIA interaction regulates VEGF-A mRNA stability and arteriogenesis. *J Exp Med* 2014;211:1957-68.
35. Kunisawa J, Gohda M, Hashimoto E, Ishikawa I, Higuchi M, Suzuki Y, et al. Microbe-dependent CD11b $^{+}$ IgA $^{+}$ plasma cells mediate robust early-phase intestinal IgA responses in mice. *Nat Commun* 2013;4:1772.
36. Inoue A, Ishiguro J, Kitamura H, Arima N, Okutani M, Shuto A, et al. TGF α shedding assay: an accurate and versatile method for detecting GPCR activation. *Nat Methods* 2012;9:1021-9.
37. Park DK, Lee YG, Park HJ. Extract of *Rhus verniciflua* bark suppresses 2,4-dinitrofluorobenzene-induced allergic contact dermatitis. *Evid Based Complement Alternat Med* 2013;2013:879696.
38. Tajima Y, Ishikawa M, Maekawa K, Murayama M, Senoo Y, Nishimaki-Mogami T, et al. Lipidomic analysis of brain tissues and plasma in a mouse model expressing mutated human amyloid precursor protein/tau for Alzheimer's disease. *Lipids Health Dis* 2013;12:68.
39. Ong PY, Ohtake T, Brandt C, Strickland I, Boguniewicz M, Ganz T, et al. Endogenous antimicrobial peptides and skin infections in atopic dermatitis. *N Engl J Med* 2002;347:1151-60.
40. Kish DD, Gorbachev AV, Parameswaran N, Gupta N, Fairchild RL. Neutrophil expression of Fas ligand and perforin directs effector CD8 T cell infiltration into antigen-challenged skin. *J Immunol* 2012;189:2191-202.
41. Kaku K, Enya K, Nakaya R, Ohira T, Matsuno R. Long-term safety and efficacy of fasiglifam (TAK-875), a G-protein-coupled receptor 40 agonist, as monotherapy and combination therapy in Japanese patients with type 2 diabetes: a 52-week open-label phase III study. *Diabetes Obes Metab* 2016;18:925-9.
42. Fujita T, Matsuoka T, Honda T, Kabashima K, Hirata T, Narumiya S. A GPR40 agonist GW9508 suppresses CCL5, CCL17, and CXCL10 induction in keratinocytes and attenuates cutaneous immune inflammation. *J Invest Dermatol* 2011;131:1660-7.
43. Mashimo H, Ohguro N, Nomura S, Hashida N, Nakai K, Tano Y. Neutrophil chemotaxis and local expression of interleukin-10 in the tolerance of endotoxin-induced uveitis. *Invest Ophthalmol Vis Sci* 2008;49:5450-7.
44. Scimone ML, Lutzyk VP, Zittermann SI, Maffia P, Jancic C, Buzzola F, et al. Migration of polymorphonuclear leukocytes is influenced by dendritic cells. *Immunology* 2005;114:375-85.
45. Marasco WA, Phan SH, Krutzsch H, Showell HJ, Feltner DE, Nairn R, et al. Purification and identification of formyl-methionyl-leucyl-phenylalanine as the major peptide neutrophil chemotactic factor produced by *Escherichia coli*. *J Biol Chem* 1984;259:5430-9.
46. van der Hoeven D, Gizewski ET, Auchampach JA. Activation of the A(3) adenosine receptor inhibits fMLP-induced Rac activation in mouse bone marrow neutrophils. *Biochem Pharmacol* 2010;79:1667-73.
47. Cassimeris L, Zigmond SH. Chemoattractant stimulation of polymorphonuclear leukocyte locomotion. *Semin Cell Biol* 1990;1:125-34.
48. Mizgerd JP, Kubo H, Kutkoski GJ, Bhagwan SD, Scharffetter-Kochanek K, Beudet AL, et al. Neutrophil emigration in the skin, lungs, and peritoneum: different requirements for CD11/CD18 revealed by CD18-deficient mice. *J Exp Med* 1997;186:1357-64.
49. Cattani F, Gallese A, Mosca M, Buanne P, Biorci L, Francavilla S, et al. The role of CXCR2 activity in the contact hypersensitivity response in mice. *Eur Cytokine Netw* 2006;17:42-8.
50. Cheng DT, Ma C, Niewoehner J, Dahl M, Tsai A, Zhang J, et al. Thymic stromal lymphopoietin receptor blockade reduces allergic inflammation in a cynomolgus monkey model of asthma. *J Allergy Clin Immunol* 2013;132:455-62.
51. Hauge M, Vestmar MA, Husted AS, Ekberg JP, Wright MJ, Di Salvo J, et al. GPR40 (FFAR1)—combined Gs and Gq signaling in vitro is associated with robust incretin secretagogue action ex vivo and in vivo. *Mol Metab* 2015;4:3-14.
52. Shi G, Partida-Sanchez S, Misra RS, Tighe M, Borchers MT, Lee JJ, et al. Identification of an alternative G(α)q-dependent chemokine receptor signal transduction pathway in dendritic cells and granulocytes. *J Exp Med* 2007;204:2705-18.
53. Ridley AJ. Rho GTPase signalling in cell migration. *Curr Opin Cell Biol* 2015;36:103-12.
54. Welch HC. Regulation and function of P-Rex family Rac-GEFs. *Small GTPases* 2015;6:49-70.
55. Gross S, Gammon ST, Moss BL, Rauch D, Harding J, Heinecke JW, et al. Bioluminescence imaging of myeloperoxidase activity in vivo. *Nat Med* 2009;15:455-61.
56. Molesworth-Kenyon SJ, Oakes JE, Lausch RN. A novel role for neutrophils as a source of T cell-recruiting chemokines IP-10 and Mig during the DTH response to HSV-1 antigen. *J Leukoc Biol* 2005;77:552-9.
57. Abdel-Latif D, Steward M, Macdonald DL, Francis GA, Dinayer MC, Lacy P. Rac2 is critical for neutrophil primary granule exocytosis. *Blood* 2004;104:832-9.
58. Ingraham RH, Gless RD, Lo HY. Soluble epoxide hydrolase inhibitors and their potential for treatment of multiple pathologic conditions. *Curr Med Chem* 2011;18:587-603.
59. Zhou SF, Liu JP, Chowbay B. Polymorphism of human cytochrome P450 enzymes and its clinical impact. *Drug Metab Rev* 2009;41:89-295.
60. Schwarz D, Kisselev P, Ericksen SS, Szklarz GD, Chernogolov A, Honeck H, et al. Arachidonic and eicosapentaenoic acid metabolism by human CYP1A1: highly stereoselective formation of 17(R),18(S)-epoxyeicosatetraenoic acid. *Biochem Pharmacol* 2004;67:1445-57.
61. Lucas D, Goullitquer S, Marienhagen J, Fer M, Dreano Y, Schwaneberg U, et al. Stereoselective epoxidation of the last double bond of polyunsaturated fatty acids by human cytochromes P450. *J Lipid Res* 2010;51:1125-33.
62. Arnold C, Markovic M, Blosser K, Wallukat G, Fischer R, Dechend R, et al. Arachidonic acid-metabolizing cytochrome P450 enzymes are targets of ω -3 fatty acids. *J Biol Chem* 2010;285:32720-33.
63. Oyoshi MK, He R, Li Y, Mondal S, Yoon J, Afshar R, et al. Leukotriene B $_4$ -driven neutrophil recruitment to the skin is essential for allergic skin inflammation. *Immunity* 2012;37:747-58.
64. Keijsers RR, Hendriks AG, van Erp PE, van Cranenbroek B, van de Kerckhof PC, Koenen HJ, et al. In vivo induction of cutaneous inflammation results in the accumulation of extracellular trap-forming neutrophils expressing ROR γ t and IL-17. *J Invest Dermatol* 2014;134:1276-84.
65. Miyamoto J, Mizukure T, Park SB, Kishino S, Kimura I, Hirano K, et al. A gut microbial metabolite of linoleic acid, 10-hydroxy-cis-12-octadecenoic acid, ameliorates intestinal epithelial barrier impairment partially via GPR40-MEK-ERK pathway. *J Biol Chem* 2015;290:2902-18.
66. Barbara G, Zecchi L, Barbaro R, Cremon C, Bellacosa L, Marcellini M, et al. Mucosal permeability and immune activation as potential therapeutic targets of probiotics in irritable bowel syndrome. *J Clin Gastroenterol* 2012;46(suppl):S52-5.
67. Arita M, Ohira T, Sun YP, Elangovan S, Chiang N, Serhan CN. Resolvin E1 selectively interacts with leukotriene B $_4$ receptor BLT1 and ChemR23 to regulate inflammation. *J Immunol* 2007;178:3912-7.

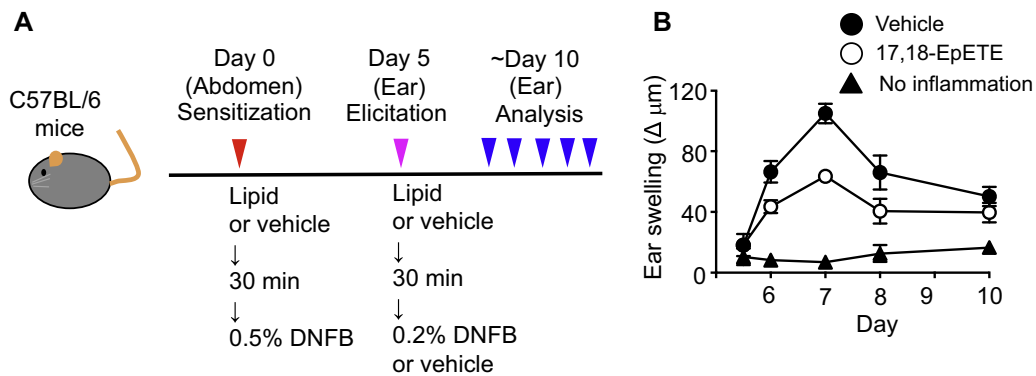


FIG E1. Chronologic analysis of ear swelling in DNFB-induced contact hypersensitivity in mice. **A**, Experimental protocol for induction of contact hypersensitivity by DNFB and treatment with 17,18-EpETE. At both the sensitization and elicitation phases, mice were injected intraperitoneally with either 17,18-EpETE or vehicle at 30 minutes before application of DNFB. Ear thickness was evaluated by using a micrometer. Ear swelling was calculated as follows: (Ear thickness [in micrometers] after DNFB application) – (Ear thickness [in micrometers] before DNFB application) = Δ micrometers. **B**, Ear swelling was analyzed at the indicated time points. Data are expressed as means \pm SEMs (n = 4 to 24).

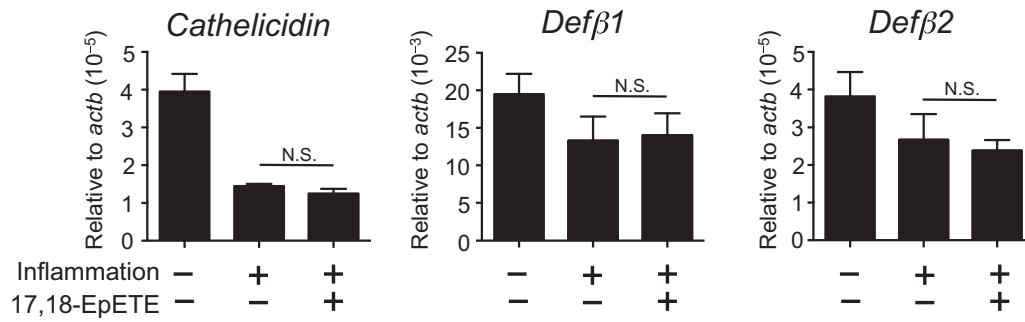


FIG E2. 17,18-EpETE does not affect gene expression of various antimicrobial peptides. Ear tissues were obtained on day 7 and homogenized for isolation of mRNA, and quantitative RT-PCR analysis was performed to measure cathelicidin, defensin-β1, and defensin-β2 expression, which was normalized to that of *Actb*. Data are expressed as means ± SDs (3 replicate measurements) and representative of 2 independent experiments. Statistical significance was evaluated by using ordinary 1-way ANOVA. *N.S.*, Not significant.

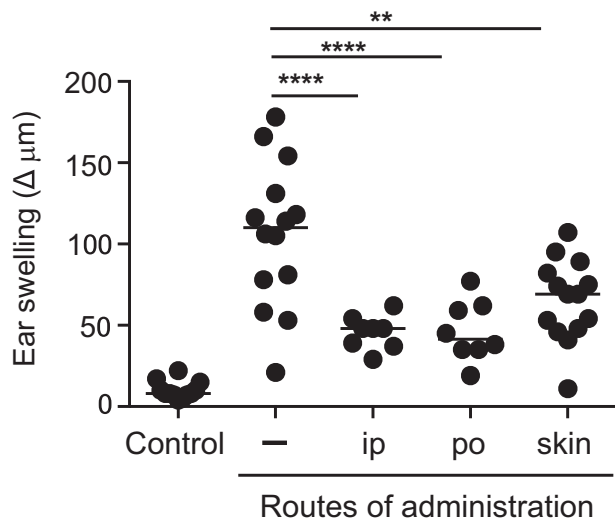


FIG E3. 17,18-EpETE is effective not only through the intraperitoneal route but also through the oral and topical routes. At both the sensitization and elicitation phases, mice were treated with 17,18-EpETE (dose per time point: 100 ng administered intraperitoneally [*ip*] or 1 μg administered orally [*po*] or topically [*skin*]) through the indicated route at 30 minutes before DNFB application. Ear swelling was evaluated on day 7. Data are combined from 3 independent experiments, and each *point* represents data from an individual mouse. Center values indicate medians. Statistical significance was evaluated by using 1-way ANOVA: ** $P < .01$ and **** $P < .0001$.

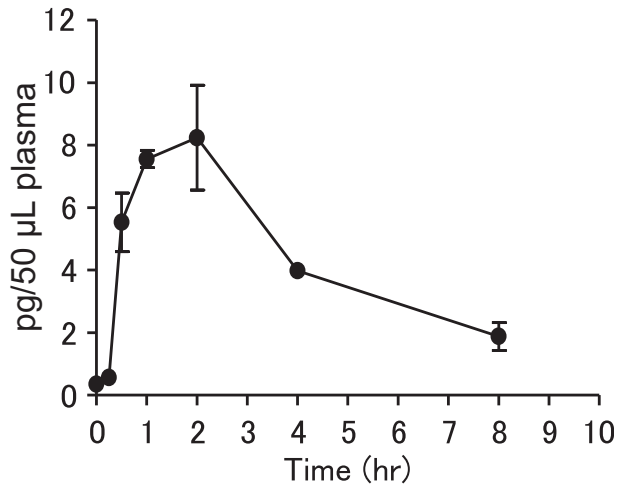


FIG E4. Pharmacokinetic analysis of 17,18-EpETE. Plasma samples were collected at indicated time points after oral administration of 17,18-EpETE. The amount of 17,18-EpETE was quantified by using liquid chromatography–tandem mass spectrometry. Data are expressed as means \pm SDs ($n = 3$).

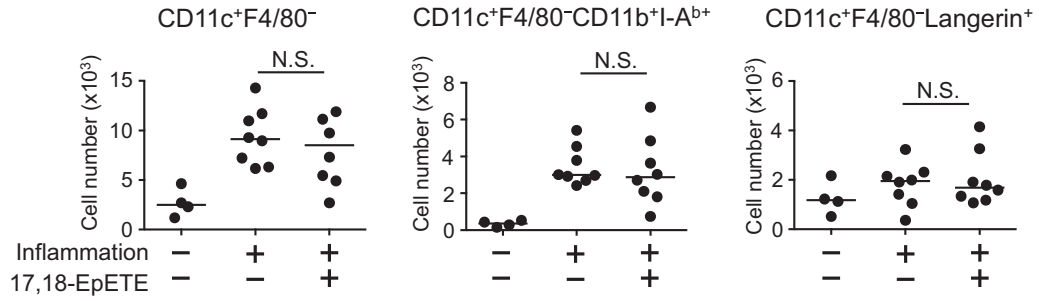


FIG E5. Numbers of DCs in inflamed skin are unchanged by 17,18-EpETE. Mice were injected intraperitoneally with either 17,18-EpETE or vehicle on days 0 and 5 at 30 minutes before DNFB application. Ear samples were obtained on day 7. Numbers of DCs were calculated by using total cell numbers and flow cytometric data of indicated DC populations. Data are representative of 2 independent experiments, and each *point* represents data from an individual mouse. Center values indicate medians. Statistical significance was evaluated by using 1-way ANOVA. *N.S.*, Not significant.

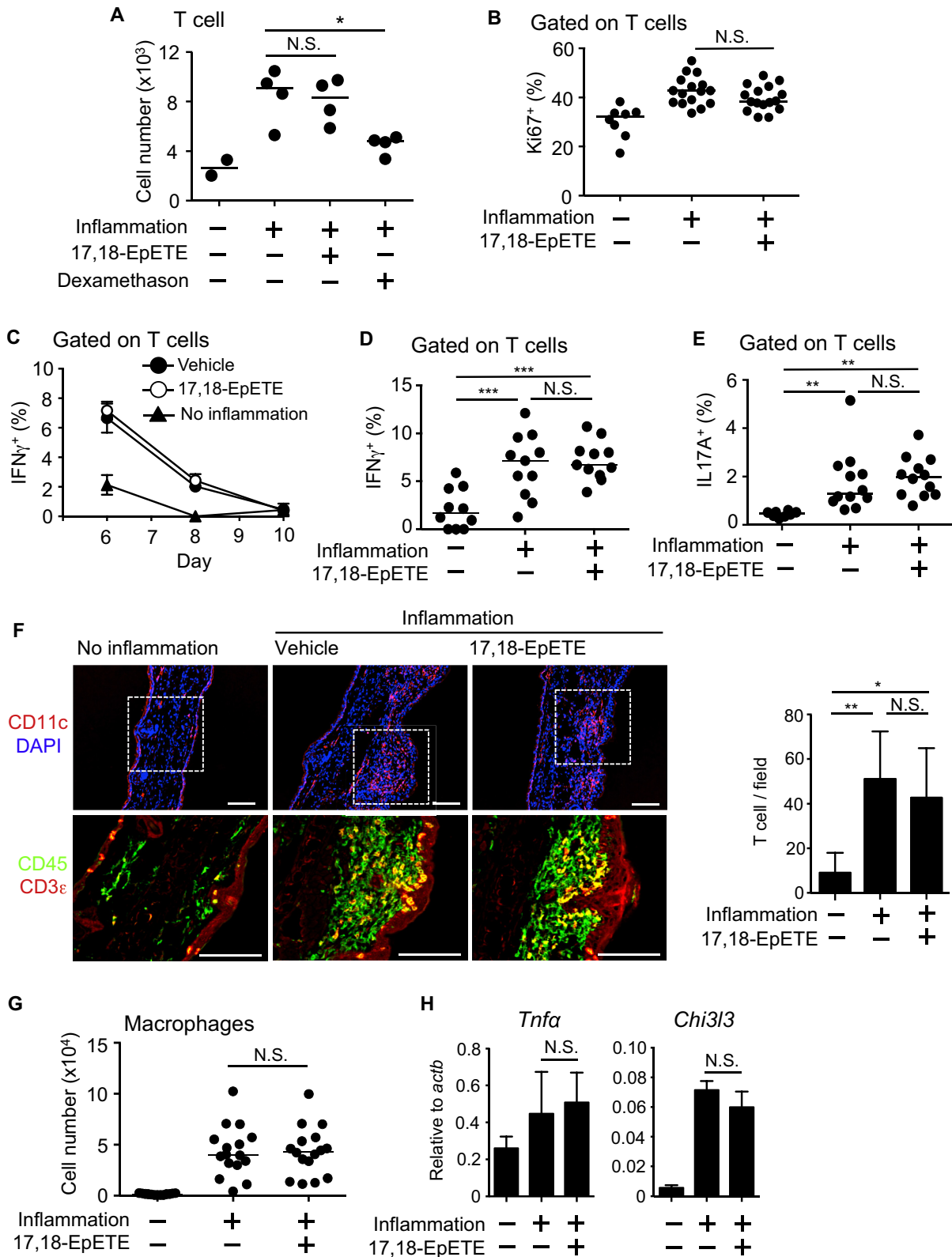


FIG E6. ISALT formation and T-cell activation are not disrupted by 17,18-EpETE. **A**, Mice were treated topically with either 17,18-EpETE, dexamethasone, or vehicle on days 0 and 5 at 30 minutes before DNFB application. Ear samples were obtained on day 7. Numbers of CD45⁺CD3 ϵ ⁺ live T cells were calculated by using total cell numbers and flow cytometric data. Data are representative of 2 independent experiments, and each *point* represents data from an individual mouse. Center values indicate medians. Statistical significance was evaluated by using 1-way ANOVA: **P* < .05. *N.S.*, Not significant. **B**, Mice were injected

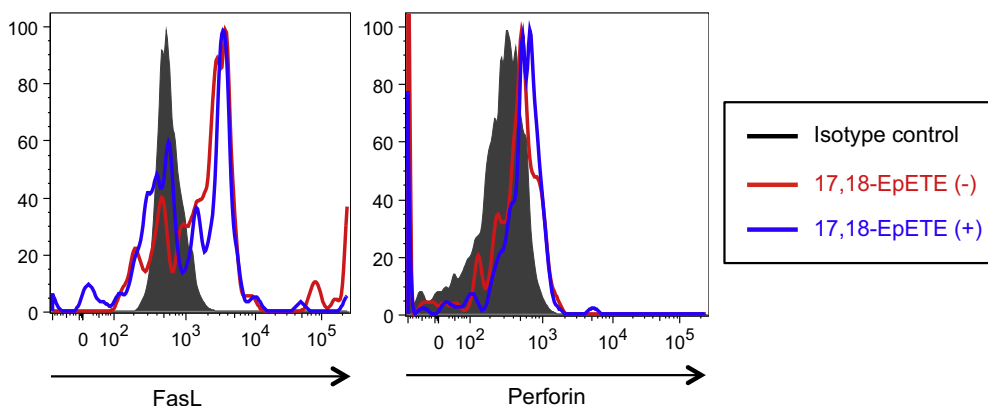


FIG E7. 17,18-EpETE does not affect expression of FasL and perforin in neutrophils. Mice were injected intraperitoneally with either 17,18-EpETE or vehicle on days 0 and 5 at 30 minutes before DNFB application. Ly6G⁺CD11b⁺ neutrophils harvested from the skin on day 6 were examined by using flow cytometry to determine the expression of FasL and perforin. Similar results were obtained in 2 independent experiments.

intraperitoneally with either 17,18-EpETE or vehicle on days 0 and 5 at 30 minutes before DNFB application. Ear samples were obtained on day 7. The percentage of Ki67⁺ cells in the CD3e⁺ live T-cell fraction was shown. Data are combined from 3 independent experiments, and each *point* represents data from individual mice. Center values indicate medians. Statistical significance was evaluated by using 1-way ANOVA. *N.S.*, Not significant. **C**, Mice were injected intraperitoneally with either 17,18-EpETE or vehicle on days 0 and 5 at 30 minutes before DNFB application. Ear samples were obtained at indicated time points. Percentages of IFN-γ⁺ cells in the CD45⁺ T-cell receptor (TCR) β⁺CD4⁻ live T-cell fraction are shown. Data are expressed as means ± SEMs (n = 4 to 11). **D** and **E**, Mice were injected intraperitoneally with either 17,18-EpETE or vehicle on days 0 and 5 at 30 minutes before DNFB application. Ear samples were obtained and analyzed by means of flow cytometry on day 6 for IFN-γ⁺ cells in the CD45⁺TCRβ⁺CD4⁻ live T-cell fraction (see Fig E6, *D*) or on day 7 for IL-17A⁺ cells in the CD3e⁺ live T-cell fraction (see Fig E6, *E*). Data are combined from 3 independent experiments, and each *point* represents data from an individual mouse. Center values indicate medians. Statistical significance was evaluated by using 1-way ANOVA. *N.S.*, Not significant. **F**, Mice were injected intraperitoneally with either 17,18-EpETE or vehicle on days 0 and 5 at 30 minutes before DNFB application. Ear samples were obtained on day 7, and frozen sections were stained with the indicated antibodies and reagents. Data are representative of 5 independent experiments. *Scale bars* = 100 μm. Number of CD45⁺CD3e⁺ T cells per field (magnification ×200) was counted, and data are expressed as means ± SDs (n = 5-13). Statistical significance was evaluated by using 1-way ANOVA: **P* < .05 and ***P* < .01. *N.S.*, Not significant. **G**, Mice were injected intraperitoneally with either 17,18-EpETE or vehicle on days 0 and 5 at 30 minutes before DNFB application. Ear samples were obtained on day 7, and numbers of F4/80⁺CD11b⁺ macrophages in the skin were calculated by using flow cytometry. Data are combined from 3 independent experiments, and each *point* represents data from an individual mouse. Center values indicate medians. Statistical significance was evaluated by using 1-way ANOVA. *N.S.*, Not significant. **H**, Mice were injected intraperitoneally with either 17,18-EpETE or vehicle on days 0 and 5 at 30 minutes before DNFB application. Ear samples were obtained on day 7, and F4/80⁺CD11b⁺ macrophages were isolated for quantitative RT-PCR analysis of M1 and M2 marker expression, which was normalized to that of *Actb*. Data are expressed as means ± SDs (3 replicate measurements) and representative of 2 independent experiments. Statistical significance was evaluated by using 1-way ANOVA. *N.S.*, Not significant.

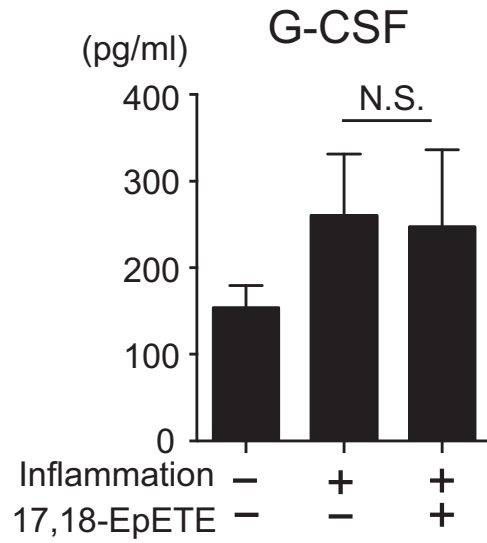


FIG E8. 17,18-EpETE does not affect the amount of G-CSF in serum. Mice were injected intraperitoneally with either 17,18-EpETE or vehicle on days 0 and 5 at 30 minutes before DNFB application. Serum samples were obtained on day 7 and analyzed by means of ELISA for measurement of G-CSF. Data are expressed as means \pm SDs (n = 5 to 8). Statistical significance was evaluated by using 1-way ANOVA. *N.S.*, Not significant.

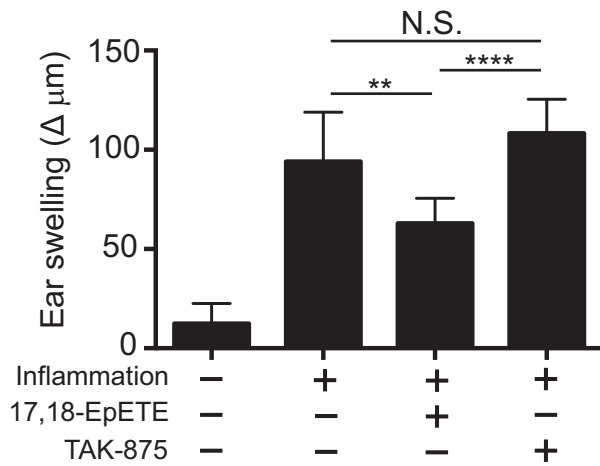


FIG E9. Contact hypersensitivity is ameliorated by 17,18-EpETE but not TAK-875. Mice were injected intraperitoneally with either 17,18-EpETE or TAK-875 on days 0 and 5 at 30 minutes before DNFB application. Ear swelling was analyzed on day 7. Data are combined from 2 independent experiments and expressed as means \pm SDs (n = 8). Statistical significance was evaluated by using 1-way ANOVA: ** $P < .01$ and **** $P < .0001$. *N.S.*, Not significant.

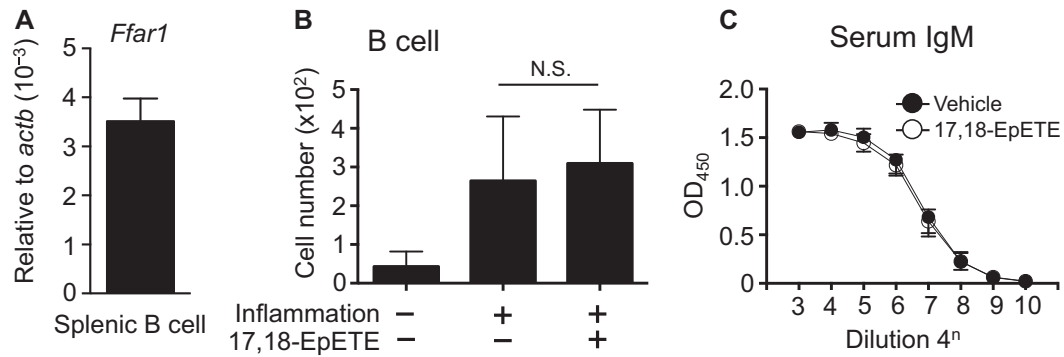


FIG E10. 17,18-EpETE does not affect B-cell function. **A**, $CD45^+B220^+CD19^+$ live B cells were isolated from spleens, and RT-PCR analysis was performed to examine gene expression of the *Ffar1* gene. Data are expressed as means \pm SEMs ($n = 7$). **B**, Mice were injected intraperitoneally with either 17,18-EpETE or vehicle on days 0 and 5 at 30 minutes before DNFB application. Ear samples were obtained on day 7. Numbers of $CD45^+B220^+CD19^+$ live B cells were calculated by using total cell numbers and flow cytometric data. Data are expressed as means \pm SDs ($n = 2-4$). Statistical significance was evaluated by using 1-way ANOVA. *N.S.*, Not significant. **C**, Mice were injected intraperitoneally with either 17,18-EpETE or vehicle on days 0 and 5 at 30 minutes before DNFB application. Serum samples were obtained on day 7 and analyzed by means of ELISA for the measurement of IgM. Data are combined from 3 independent experiments and expressed as means \pm SDs ($n = 12$).

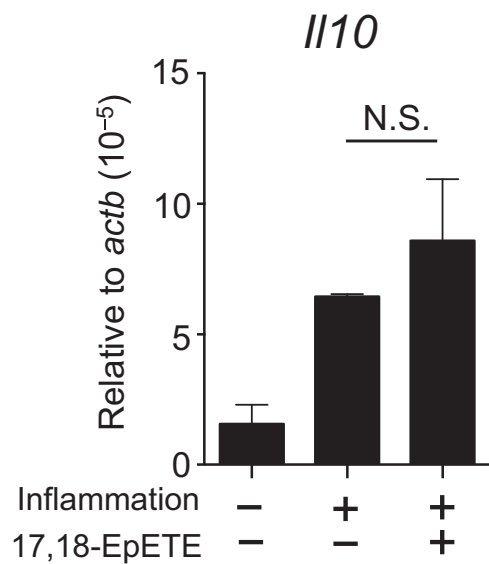


FIG E11. 17,18-EpETE does not affect gene expression of *I/10* in inflamed skin. Mice were injected intraperitoneally with either 17,18-EpETE or vehicle on days 0 and 5 at 30 minutes before DNFB application. Ear samples were obtained on day 7 and homogenized for isolation of mRNA, and quantitative RT-PCR analysis was performed to measure *I/10* expression, which was normalized to that of *Actb*. Data are expressed as means \pm SDs (3 replicate measurements) and representative of 2 independent experiments. Statistical significance was evaluated by using 1-way ANOVA. *N.S.*, Not significant.

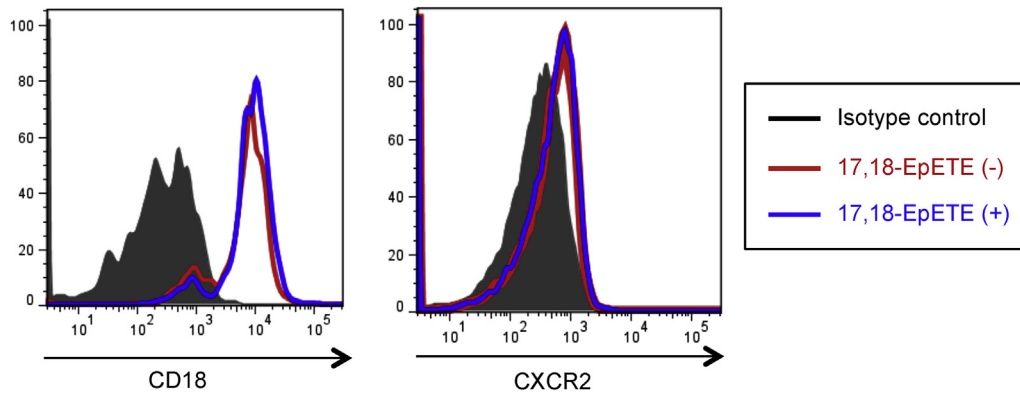


FIG E12. 17,18-EpETE does not affect expression of CD18 or CXCR2 on neutrophils. Ly6G⁺CD11b⁺ neutrophils harvested from skins and spleens were examined by using flow cytometry for expression of CD18 and CXCR2, respectively, in the murine model of DNFB-induced contact hypersensitivity. Similar results were obtained in 2 independent experiments.